Chinese Journal of Aeronautics, (2015),28(2): 327–345

Chinese Society of Aeronautics and Astronautics
& Beihang University

Chinese Journal of Aeronautics

cja@buaa.edu.cn
www.sciencedirect.com

REVIEW ARTICLE (INVITED)

Transfer element method with application to acoustic design of aeroengine nacelle

Wang Xiaoyu [a,b], Sun Xiaofeng [a,b,*]

[a] School of Energy and Power Engineering, Beihang University, Beijing 100191, China
[b] Collaborative Innovation Center for Advanced Aero-Engine, Beijing 100191, China

Received 19 December 2014; revised 30 December 2014; accepted 30 January 2015
Available online 3 March 2015

KEYWORDS

Duct acoustics;
Equivalent surface source method;
Interaction of sound source and acoustic treatment;
Acoustic liner;
Three-dimensional lifting surface theory;
Transfer element method;
Aeroengine noise

Abstract In the present survey, various methods for the acoustic design of aeroengine nacelle are first briefly introduced along with the comments on their advantages and disadvantages for practical application, and then detailed analysis and discussion focus on a kind of new method which is called "transfer element method" (TEM) with emphasis on its application in the following three problems: turbomachinery noise generations, sound transmission in ducts and radiation from the inlet and outlet of ducts, as well as the interaction between them. In the theoretical frame of the TEM, the solution of acoustic field in an infinite duct with stator sound source or liner is extended to that in a finite domain with all knows and unknowns on the interface plane, and the relevant acoustic field is solved by setting up matching equation. In addition, based on combining the TEM with the boundary element method (BEM) by establishing the pressure and its derivative continuum conditions on the inlet and outlet surface, the sound radiation from the inlet and outlet of ducts can also be investigated. Finally, the effects of various interactions between the sound source and acoustic treatment have been discussed in this survey. The numerical examples indicate that it is quite important to consider the effect of such interactions on sound attenuation during the acoustic design of aeroengine nacelle.

1. Introduction

As the main noise source of modern commercial aircraft, the acoustic design of aeroengine has received more and more attention along with increasingly stringent requirement for environmental protection.[1] Therefore, how to further reduce aeroengine noise by all means has long been a problem of great importance. It is well-known that the best way is to control the noise sources themselves[2,3] at the design phase of aeroengine and suppress its propagation in ducts.[4–6] In fact, it is noted that aeroengine noise is generated by either an internal or an external source. The externally generated noise is due mainly

* Corresponding author. Tel.: +86 10 82317408.
E-mail addresses: bhwxy@buaa.edu.cn (X. Wang), sunxf@buaa.edu.cn (X. Sun).
Peer review under responsibility of Editorial Committee of CJA.

Production and hosting by Elsevier

http://dx.doi.org/10.1016/j.cja.2015.02.005
1000-9361

to the jet exhaust. The internally generated noise is due primarily to the rotating turbomachinery blades and to the combustion process. To achieve lower specific fuel consumption, future aircraft engines are expected to have bypass ratios in the range of 12–15.[1] This results in a reduction of the jet noise to relatively insignificant proportions, but leads to an increase of the fan noise. If there is no acoustic treatment to control the noise propagation, some tests show that the overall noise level of such engines is greater than the noise level of low bypass engines and consists of a broad band spectrum and high-pitched discrete frequency components.[7] The internal flow field past the blades is generally unsteady due to the presence of upstream blades and vanes and viscous wake. The interaction of this unsteady flow and the moving blades produces upstream and downstream traveling pressure waves (acoustic modes) with BPF (Blade Passing Frequency) as its frequency characteristics. Some of these modes decay naturally (cut-off modes), while the others (cut-on modes) need to be suppressed by acoustically treating the engine ducts.[8] The latter is just the main objective of the acoustic design of aeroengine nacelle. To achieve noise reductions in the nacelle as much as possible, the acoustic treatment must be optimized, and in addition, how to include the effect of the interaction between the sound source and acoustic treatment on noise attenuation is also a problem of concern.

It is noted that considerable work has been conducted for the prediction of the sound radiation from a lined duct over the last decade, including the boundary integral equation method (BIEM) or boundary element method (BEM),[9–13] the finite element method (FEM)[14–18] and the numerical simulation method based on computational aeroacousitc (CAA) technique.[19–22] These methods are playing a diverse role at different stages of the acoustic design. For the determination of final design parameters, it is necessary to use the numerical simulation tools as accurate as possible to check the results provided that the relevant computing cost is affordable. However, for the purpose of preliminary design considerations, an acoustic engineer must conduct a large number of parametric studies. In this situation, it is required to provide fast, useful and reliable tools to acoustic engineers.

The purpose of the present paper is to critically survey the state-of-the art regarding the methods of determining the sound attenuation, source-acoustic treatment interaction and sound radiation from the inlet and exhaust of aeroengine. Especially, emphasis will be put on how to use a kind of new strategy, transfer element method (TEM) to realize the prescribed noise reduction objective at the preliminary phase of the acoustic design of aeroengine nacelle.

2. Physical pictures and computational models

As shown in Fig. 1, in order to control the noise propagation and radiation from aeroengine nacelle efficiently, various acoustic treatments have to be installed in all the available places, such as inlet and outlet of nacelle, even the duct surface between rotor and stator. In the past several decades, many sound propagation models have been developed to calculate the noise attenuation. In general, different acoustic treatments are used to realize an optimal attenuation for various sound sources with broad frequency range. Obviously, different liners will interact with each other due to discontinuous impedance distribution, and the presence of the rotor and stator as sound source or the reflection of nozzle could also interact with the acoustic liner. In fact, a good model for the acoustic design of the aeroengine nacelle is to include such interactions as much as possible in order to realize more accurate description to the special sound environment as Fig. 1. This is indeed not an easy task. Fig. 2 just shows the complex process toward this objective.

At the preliminary stage of acoustic liner design, in order to obtain the structure parameters of liner as soon as possible, it is necessary to introduce a simplified calculation model with the assumptions like mean flow, infinite duct and strength-fixed sound sources. At this stage, some famous simplified models, such as mode-matching approach (MMA) and BIEM can be used to estimate sound attenuation for different liner combinations. However these design models can still not satisfy the current requirement of acoustic treatment design for modern turbofan aeroengine. Therefore, it is indeed required to have a kind of new model to consider the effect of non-uniform duct, complex flow and the interaction between sound source and various liners on the sound attenuation. On the other hand, more elaborate numerical calculation method like CAA is also quite important due to its capability to include any complex factors. However, since huge time and computational cost are inevitable for this regard, it is very difficult to use it to conduct parametric study with the requirement of fast implementation. So, from a practical view of point, a fast method which can be used to optimize all design parameters of acoustic treatment with fewer restrictions is still required.

In addition, the impedance model is also an important factor for liner design, but in the present survey, we only suppose that the impedance description can be available, such as Ingard's model[24] and Jing et al.'s model.[25–28] So, emphasis will be placed on the various propagation models in ducts, and especially on the connection between the acoustic attenuation and liner structure parameters.

As discussed above, in order to satisfy the requirement of acoustic liner design for modern turbofan nacelle, we need a new model to solve the following problems: (a) the model can be used in the preliminary design stage for calculating the sound propagation in duct and sound radiation from the inlet and exhaust; (b) the model must include more effect of liner design such as non-uniform flow and varying cross-sectional duct; (c) the model can consider the effect of the interaction between the sound sources and acoustic treatments. For these three purposes, we will first review several famous existing models like MMA and BIEM, and then focus on introducing how TEM is developed to solve the sound propagation problem in aeroengine nacelle with the above three main features.

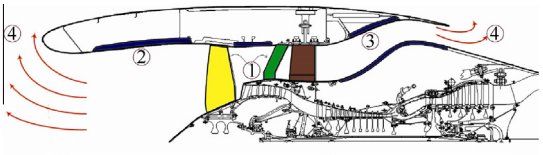

Fig. 1 Schematic of simplified aeroengine acoustic model.

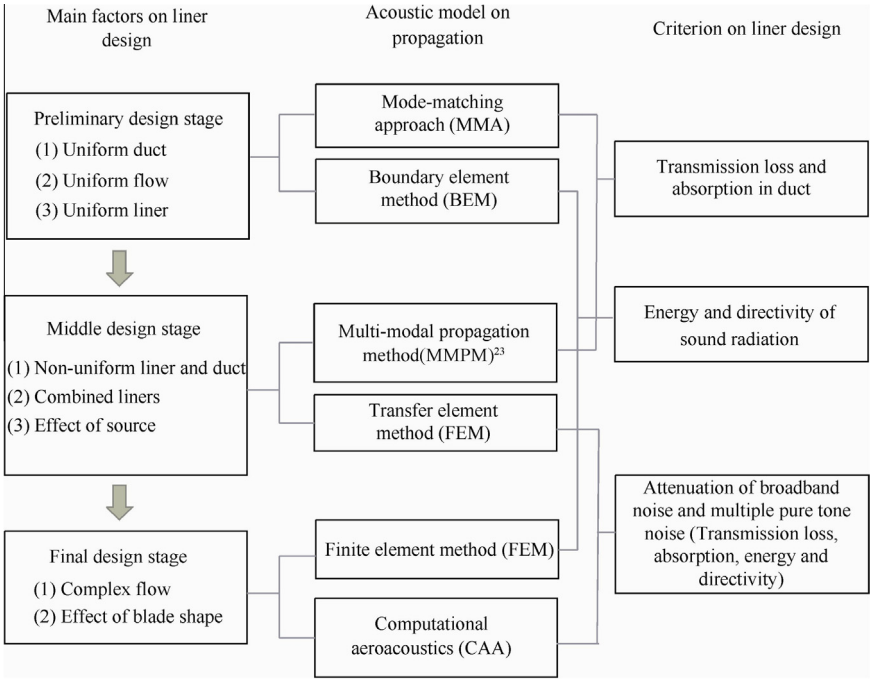

Fig. 2 Block diagram of requirements of liner design. (See above-mentioned references for further information.)

2.1. MMA

Acoustic engineers only designed the acoustic treatment via calculating the eigenvalue of infinitely long acoustic liner before MMA was published.[29–31] It is so difficult to compute the eigenvalue that it is necessary to check the resolution through the experiment. In 1974, Zorumski[32] developed the MMA to consider the sound propagation in the multisectioned ducts which are interconnected. Zorumski tried to solve all acoustics problems including sound generation in, transmission through and radiation from duct, as shown in Fig. 3. However, the sound source on the blades was regarded as the spinning point source without considering the interaction between the sound field and the blade unsteady loading. Aimed at the sound propagation, this method divides the acoustic pressure into a sum of multimode.

As shown in Fig. 4, the infinite duct solution must be generalized to account for the effects of some finite sections, and relationships must be developed to account for the acoustic coupling between these sections. Firstly in order to define the acoustic field in terms of wave amplitudes, we can write sound pressure by the following equation:

$$p'_m(r,z)=\sum_{\mu=1}^{\infty}\left[A_{m\mu}^{+j}\psi_{m\mu}^{+j}(k_{m\mu}r)e^{i\gamma_{m\mu}^{+j}(z-z^j)}-A_{m\mu}^{-j}\psi_{m\mu}^{-j}(k_{m\mu}r)\mathrm{e}^{i\gamma_{m\mu}^{-j}(z-z^j)}\right] \tag{1}$$

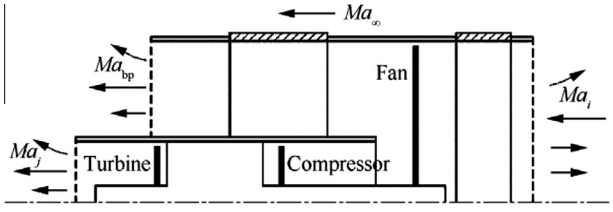

Fig. 3 Schematic of engine acoustic model.

where $A_{m\mu}^{+j}$ and $A_{m\mu}^{-j}$ are the amplitudes of the acoustic modes at z^j; $\psi_{m\mu}(r)$ denotes the eigenfunction of the cross section in duct and $k_{m\mu}$ is the eigenvalue; $\gamma_{m\mu}$ expresses the axial wave number. Therefore, the wave generation, transmission and reflection effects at the interface $j-k$ can be represented by matrix equations as

$$\begin{aligned}[A_{m\mu}^{+k}]&=[T_{m\mu\nu}^{+k+j}][A_{m\nu}^{+j}]+[R_{m\mu\nu}^{+k-k}][A_{m\nu}^{-k}]+[Q_{m\mu}^{+k}]\\ [A_{m\mu}^{-j}]&=[T_{m\mu\nu}^{-j-k}][A_{m\nu}^{-k}]+[R_{m\mu\nu}^{-j+j}][A_{m\nu}^{+j}]+[Q_{m\mu}^{-j}]\end{aligned} \tag{2}$$

where the factors $\boldsymbol{R}$ and $\boldsymbol{T}$ are called the reflection coefficient and transmission coefficient of interface, respectively; $[Q_{m\mu}^{+k}]$ indicates the source terms for the forward waves in the section k. Utilizing the matching condition on the interface $j-k$, we can obtain

$$\begin{cases}[T_{m\mu\nu}^{+k+j}]=\left[W_{m\mu\nu}^{-j+k}\right]^{-1}[W_{m\mu\nu}^{-j+j}]\\ [R_{m\mu\nu}^{+k-k}]=\left[W_{m\mu\nu}^{-j+k}\right]^{-1}[W_{m\mu\nu}^{-j-k}]\end{cases} \tag{3}$$

where $[W_{m\mu\nu}^{-j+k}]$ is the function of $[I_{m\mu\nu}^{-j+k}]$. And

$$I_{m\mu\nu}^{-j+k}=\int_a^b r\psi_{m\mu}^{j}(r)\psi_{m\nu}^{k}(r)\mathrm{d}r \tag{4}$$

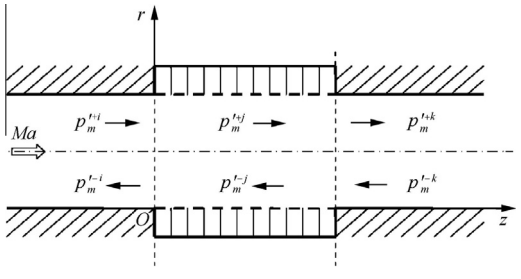

Fig. 4 Transmission wave and reflection wave in duct by utilizing MMA.

Obviously, in order to obtain the transmission and reflection coefficient, the most important thing is to calculate the eigenvalue and eigenfunction of these two adjacent sections. It is easy to obtain the eigenvalue if only there is hard wall in the duct. However, if the impedance boundary conditions are different between these two elements, it becomes very difficult to solve the eigenvalue in Eq. (4) in which the modes are not orthogonal. The reason is that we have described the wall boundary condition as a transcendental equation with the help of the concept of acoustic impedance instead of directly considering the sound propagation inside the liner. For example, in the rectangular duct with one-side liner, we can set up the impedance equation as

$$\tan(k_x l) = \frac{-\mathrm{i}k_0\beta}{k_x}\left(1 - Ma\frac{k_z}{k_0}\right)^2 \tag{5}$$

where k_x and k_z refer to the wave numbers for each duct propagation mode in x and z direction; $k_0 = \omega/c_0$ and $\beta^2 = 1 - Ma^2$, ω is angular frequency, c_0 is local sound speed, Ma is the Mach number of uniform flow. Unfortunately, there are lots of numerical instability and mode jump phenomena under this kind of equations. This eigenvalue equation derived from the impedance condition is usually solved by Eversman's integration method[33,34], in which a nonlinear ordinary differential equation (ODE) is adopted via introducing a parameter perturbation to the transcendental algebraic equation. There is singularity at the lowest-order mode, i.e., the plane wave, in the OED derived by Eversman's method for both rectangular and circular ducts. This problem has been solved by a homotopy method developed by Sun et al.[35] until 2007. So far, MMA is still one of the most efficient methods of liner design.

As mentioned above, in Zorumski's model, he hopes to solve all the acoustic problems involved in sound generation in, transmission through and radiation from duct systems. In this model, however, it is really difficult to give a uniform equation including sound source and liner because the eigenvalue and eigenfunction of soft wall have been used. On the other hand, there are some inextricable problems to calculate the sound radiation from the duct since it is required to input the mode reflection coefficient of the engine inlet or exhaust duct termination planes via both theoretical method and experimental method.[36,37] Moreover, the MMA only considers very simple conditions, i.e., uniform mean flow, and uniform duct. As shown in Fig. 2, using this model, we cannot calculate the sound radiation form duct without mode sound reflection coefficient at the end of duct. To overcome these difficulties, it is required to set up a combined equation including both sound propagation in and sound radiation from ducts in order to simultaneously obtain the acoustic radiation field.

2.2. BIEM

In order to better understand the effect of aeroengine noise on the acoustic environment in the cabin and airport, acoustic engineers are eager to predict the far field acoustic characteristics including both amplitude and directivity of radiation.

At first, Wiener–Hopf method was used to solve this problem assuming that the duct has a prescribed length-diameter ratio, to obtain analytical solution;[38,39] however, the approximation is too far away from practical application. In 1995, Myers[9,10] presented the boundary integral equation of sound radiation from duct with spinning point source and liner by applying Ffowcs Williams–Hawkings equation, which assumed that length of liner is equal to duct. Therefore Myers's method may also be considered to a kind of approximation to the practical problem. Later on Dunn et al.[11,40] developed different kinds of BEM model, which considered the effect of the multi-segment liner with arbitrary impedance distribution in the duct. The boundary integral equation is a fast method because it establishes a unified equation including both duct sound propagation and sound radiation. In this method, it is unnecessary to calculate the eigenvalue of impedance wall, so BEM has become one of the most effective and powerful tools of the acoustic design of aeroengine nacelle.

After that, Yang and Wang[41] developed a direct boundary element, which could calculate the effect of non-uniform impedance in circumferential direction and the scarf inlet engine. This method overcomes some calculating difficulties due to the complex singularity treatment on the impedance wall and is easily used to analyze the effect of various geometrical and aerodynamic parameters on sound field.

In this model, the acoustic fields are split into two parts, one is inside of the duct, the other one is outside of the duct, and these two parts are related by the continuing condition on the duct terminal surfaces. As shown in Fig. 5, the uncompacted source and non-uniform liner can be included.

The governing equation without mean flow in frequency domain can be written as

$$\left[k_0^2 + \frac{1}{r}\cdot\frac{\partial}{\partial r}\left(r\frac{\partial}{\partial r}\right) + \frac{1}{r^2}\cdot\frac{\partial^2}{\partial\varphi^2} + \frac{\partial^2}{\partial z^2}\right]p' = 0 \tag{6}$$

The Green's function of three-dimensional Helmholtz equation is

$$G = \frac{\mathrm{e}^{-\mathrm{i}kR}}{4\pi R} \tag{7}$$

where

$$R = \sqrt{r^2 - r'^2 - 2rr'\cos(\varphi - \varphi') + (z - z')^2} \tag{8}$$

So we can obtain the total acoustic pressure

$$p'_q = \int\left[p_q(\boldsymbol{y})\frac{\partial G(\boldsymbol{x},\boldsymbol{y})}{\partial n} - G(\boldsymbol{x},\boldsymbol{y})\frac{\partial p_q(\boldsymbol{y})}{\partial n}\right]\mathrm{d}S_q + p'_{i,q}, \quad q = 1,\ 2 \tag{9}$$

where $q = 1$ denotes the acoustic field inside the duct, and the integral surfaces are composed of duct interior surface S_1

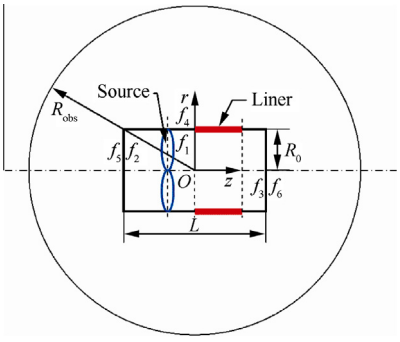

Fig. 5 Schematic of sound radiation from a duct.

including $f_1 = f_2 = f_3 = 0$. And the $p'_{i,1} = p'_i$ expresses the sound source inside the duct; $q = 2$ denotes the acoustic field outside the duct and the integral surfaces are composed of duct exterior surface S_2 including $f_4 = f_5 = f_6 = 0$. For the impedance wall and the hard wall, the boundary condition can be described as

$$\begin{cases} \frac{\partial p'_q}{\partial n} = 0 \\ \frac{\partial p'_q}{\partial n} = \frac{\mathrm{i}k}{Z_{\mathrm{im}}} p'_q \end{cases} \tag{10}$$

respectively. Here Z_{im} is the impedance on the duct wall. According to the continuing condition of pressure and its derivative on the inlet and outlet terminal surfaces, the integral equation can be given by the following forms:

$$\begin{cases} p'_q\big|_{(f_2=0)} = p'_q\big|_{(f_5=0)} \\ p'_q\big|_{(f_3=0)} = p'_q\big|_{(f_6=0)} \\ \frac{\partial p'_q}{\partial n}\big|_{(f_2=0)} = \frac{\partial p'_q}{\partial n}\big|_{(f_5=0)} \\ \frac{\partial p'_q}{\partial n}\big|_{(f_3=0)} = \frac{\partial p'_q}{\partial n}\big|_{(f_6=0)} \end{cases} \tag{11}$$

We can obtain the source items on the interior and exterior surfaces of the duct by solving these integral equations, and then obtain the acoustic field by integral expression Eq. (9). For the situation with mean flow inside and outside the duct, we suppose that the medium is at rest and the duct is moving in axial direction with Mach number $-Ma$.

It is easy to see that BIEM essentially tries to solve the scattering problem of finite length duct in the free field. As a fast method, BIEM has been used for practical liner design because it can simultaneously obtain both the acoustic attenuation and sound radiation results, as shown in Fig. 2. As mentioned above, however, this model cannot deal with more complex boundary impedance, such as non-locally reacting liner, which has been indeed considered for reducing broadband noise, since the acoustic treatment has been regarded as fixed derivative condition. On the other hand, it is unable to investigate the interactions between different kinds of liners, such as local and non-local reaction liners, and between sound sources and acoustic treatments, as shown in Fig. 2. In order to avoid this trouble, it is necessary to solve the sound propagation inside the duct by other method, such as TEM or FEM.

2.3. FEM

To predict and control sound propagation in ducts with a varying cross-sectional area is an important topic in acoustics for a long time. There are many situations occurring in practice including the liner design in the aeroengine nacelle where sound propagates in such non-uniform ducts. Both MMA and BIEM mentioned above cannot deal with this problem without making certain approximations. However, many numerical methods have been developed to handle these difficult problems, such as the FEM[16,17,42,43] and CAA[19–22] techniques. The advantages of these two methods depend on what the simulation issues are. Especially, for a sound propagation problem in duct with non-uniform flow, the linearization of the basic flow equations is generally inevitable.

Now, considering the sound propagation in duct, the governing equation can be linearized Euler equation, which can be written as

$$\frac{\partial \tilde{\boldsymbol{q}}}{\partial t} + \tilde{\boldsymbol{A}}\frac{\partial \tilde{\boldsymbol{q}}}{\partial z} + \tilde{\boldsymbol{B}}\frac{\partial \tilde{\boldsymbol{q}}}{\partial r} + \tilde{\boldsymbol{C}}\frac{\partial \tilde{\boldsymbol{q}}}{\partial \varphi} + \tilde{\boldsymbol{D}}\tilde{\boldsymbol{q}} = \boldsymbol{0} \tag{12}$$

where $\tilde{\boldsymbol{q}} = [\tilde{\rho}', \tilde{u}', \tilde{v}', \tilde{w}', \tilde{p}']^{\mathrm{T}}$ is the acoustic perturbation vector. It is noted that Eq. (12) has been used to simulate duct acoustic problem in time domain with complex flow.[22]

If we only want to know the identity of acoustic field in frequency domain, it can be expressed as elliptic equation by harmonic component assumption $\tilde{\boldsymbol{q}} = \boldsymbol{q} \cdot \mathrm{e}^{\mathrm{i}(\omega t + m\varphi)}$. For example,

$$\boldsymbol{A}\frac{\partial \boldsymbol{q}}{\partial z} + \boldsymbol{B}\frac{\partial \boldsymbol{q}}{\partial r} + \boldsymbol{C}\boldsymbol{q} = \boldsymbol{0} \tag{13}$$

This kind of equation need not be solved by time-advancement. So FEM is suitable to solve the sound propagation in frequency domain, because the FEM needs to set up the unified equation of the whole calculation region by using the principle of minimum potential energy. However, when we need consider variation of the acoustic field with time, it is necessary to solve the equation like Eq. (12) by CAA techniques.[21,44,45]

Although FEM assumes that the flow is potential flow, it is more easily implemented than CAA in both computation time and storage. The reason is that the former is only used to solve the linear Euler equation in frequency domain, which has the advantage of time-saving computation over CAA for the same approximation. Therefore, our discussion for numerical methods in duct acoustics will only focus on the application of FEM.

As a kind of numerical method, FEM can handle the issue including complex boundary and non-uniform flow along with the potential flow assumption. As shown in Fig. 6, Rienstra and Eversman[18] used this method to calculate the sound propagation in non-uniform duct like aeroengine nacelle.

The governing equations are

$$\begin{cases} \boldsymbol{\nabla} \cdot (\rho_0 \boldsymbol{V}_0) = 0 \\ \frac{1}{2}|\boldsymbol{V}_0|^2 + \frac{C}{\gamma - 1} = E \\ C^2 = \gamma \frac{p_0}{\rho_0} = \rho_0^{\gamma - 1} \end{cases} \quad \text{for mean flow field} \tag{14}$$

$$\begin{cases} \mathrm{i}\omega\rho' + \boldsymbol{\nabla} \cdot (\rho_0 \boldsymbol{\nabla}\phi + \rho' \boldsymbol{V}_0) = 0 \\ \mathrm{i}\omega\phi + \boldsymbol{V}_0 \cdot \boldsymbol{\nabla}\phi + \frac{p'}{\rho_0} = 0 \\ p' = C^2 \rho' \end{cases} \quad \text{for acoustic field} \tag{15}$$

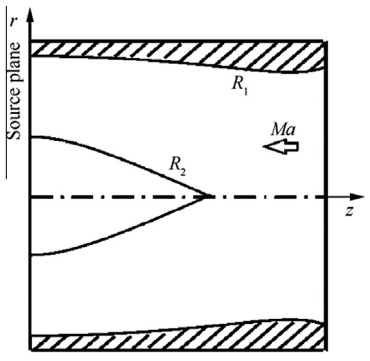

Fig. 6 Sound propagation in a non-uniform duct.

where ϕ is the velocity potential and $\tilde{\phi} = \Phi + \phi \cdot e^{i\omega t}$; $\rho_0, \boldsymbol{V}_0, p_0, C$ are the density, particle velocity, pressure and sound speed of mean flow, respectively.

For the mean flow, giving the boundary condition on the inlet and outlet terminal surfaces $\partial\Phi/\partial n = Ma_0, \Phi = 0$, we can write the Galerkin weak formulation as

$$\int_v \nabla N \cdot (\rho_0 \nabla \Phi) \mathrm{d}v = \int_S N \cdot (\rho_0 \nabla \Phi) \cdot n \mathrm{d}S \tag{16}$$

where weighting function N is from the class of continuous functions on the volume v of the duct bounded by the duct surface S, which includes the duct walls, source and terminal planes. Supposing acoustic perturbations as harmonic in time with frequency ω and harmonic in the angular coordinate θ, the weak formulation on which a finite-element model for acoustic propagation was based is

$$\begin{aligned} &\int_v \tfrac{\rho_0}{C^2}\{C^2 \nabla N \cdot \nabla \phi - (\boldsymbol{V}_0 \cdot \nabla N)(\boldsymbol{V}_0 \cdot \nabla \phi) \\ &\quad + i\omega[N(\boldsymbol{V}_0 \cdot \nabla \phi) - (\boldsymbol{V}_0 \cdot \nabla N)\phi] - \omega^2 N\phi\}\mathrm{d}v \\ &= \int_S \tfrac{\rho_0}{C^2}\{C^2 N \nabla \phi - \boldsymbol{V}_0 N(\boldsymbol{V}_0 \cdot \nabla \phi) - i\omega \boldsymbol{V}_0 N\phi\} \cdot n \mathrm{d}S \end{aligned} \tag{17}$$

The surface integral on the right-hand side of Eq. (17) is the natural boundary condition. On the terminal planes, it provides the boundary condition with the non-reflecting boundary conditions. On the lining walls the natural boundary condition is used to introduce the Myers boundary condition.[46] Ostensibly, there is no trouble in this FEM, and we can obtain the sound field as long as the noise source is determined and the computational grid is convergent. In the practice of aeroengine, however, there are a lot of acoustic waves with high mode and high frequency. This phenomenon means that we need a huge number of computational grids to simulate the sound propagation. The cost is unacceptable for non-uniform liner in circumferential direction even in the optimization of locally reacting liner. That is why it is still difficult to use FEM to calculate the radiation of sound from duct, as shown in Fig. 2. So far, this method has been used to solve the fan noise radiation from semi-infinite duct[47] without the interaction between inlet and outlet terminal planes. On the other hand, although it can consider more factors of sound generation in the duct, there are still certain difficulties to include the effect of the interaction between the second sound reflection by rotor, stator, the acoustic treatments and the end of the duct.

In summary, all of the analysis and numerical methods which are just mentioned above are useful for calculating sound propagation in lined duct. It is true that these methods have their own advantages. However, if aimed at considering the effect of the various interactions inside aeroengine nacelle as shown in Fig. 2, it is indeed indispensible to seek for a new model to suffice for the optimal acoustic design of modern turbofan nacelle.

2.4. TEM

It has been stressed that during the acoustic design of aeroengine nacelle, it is important to include the effect of more factors on the sound attenuation as much as possible, such as the reflection of duct's inlet and outlet, the non-uniform cross-section of duct and the presence of blades and vanes. Zorumski[32] attempted to calculate the sound generation, propagation and radiation in one program by using the MMA. Unfortunately, in his model, a point source model was used to replace actual distributed sources. Meanwhile, it is very difficult to reasonably obtain mode-reflection coefficients at boundary planes such as the engine inlet and exhaust. These restrictions severely affect MMA's further application in complex environment. However, in the past several years, a kind of new method, i.e., TEM[48–51] has been developed to cope with all acoustic problems mentioned above, including sound generation in, transmission through, and radiation from duct systems. Especially, with the help of TEM, we can answer some questions of concern such as the effect of sound source and the combined effect of different type of acoustic treatments on the liner design. It is worthy of noting that TEM can be used at the preliminary stage of the acoustic design in aeroengine with emphasis on a large number of parametric studies. In order to obtain an intuitive understanding into the application in the acoustic design of aeroengine nacelle, Table 1 presents a comparison between TEM and other methods.

It is worth noticing that TEM has been applied to investigating combustion instabilities[52–54] and compressor flow instabilities[55–57] due to its advantages without requiring the eigenvalue calculation due to impedance wall in duct. The relevant details for these regards can be found in Refs. [48–57].

3. TEM model and its applications

3.1. Interaction between various liners

With the application of locally reacting liner, discrete noise has been suppressed successfully. However, it is difficult to use this technology to control broadband noise due to its own characteristic of frequency response. In order to limit the noise radiation from the inlet and outlet ducts efficiently, the application of combined acoustic liner has become inevitable. It is naturally required to know how these combined liners interact with each other, and how they enhance the frequency range of sound attenuation. In this section, a model will be presented to study such interactions.

Table 1 Comparison between TEM and other methods.

Method	Sound source	Acoustic treatment		Non-uniform duct and liner	Sound radiation from duct	Interaction between sound source and liner
		Local liner	Non-local liner			
MMA		✓			✓ + BEM	
BEM		✓			✓	
FEM		✓	✓	✓		
MMPM		✓	✓	✓		
TEM	✓	✓	✓	✓	✓ + BEM	✓

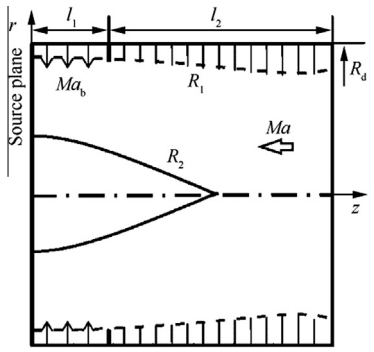

Fig. 7 Schematic of combination of locally and non-locally reacting liners with flow.

Considering the characteristic of sound spectrum in aeroengine, the combined liner consisting of locally and non-locally reacting liner has been used for suppressing the discrete noise and the broadband noise, as shown in Fig. 7. In this paper we will build a basic solution for sound propagation in finite domain or a transfer element. Based on the different interface match conditions of each transfer element, the discussion of sound propagation in lined duct with multi-section liner will be given.

As mentioned in the introduction, we want to establish a new method including the interaction between various acoustic treatments. Consequently, there are two key factors to be addressed in the new method for liner element. Firstly, we need to keep the orthogonal properties of the eigenfunction. Secondly, in order to set up matching equations on the interface, it is necessary to give the explicit expressions for the solution of both standing and scattering waves. According to scattering theory, we can regard the liner as monopole source[58], so the orthogonal properties still remain. As for the second point, we will set up the relationship between source and field in the integral equation on the liner surface.

As shown in Fig. 8, considering the interaction between the liner and acoustic field inside the element, we divide the duct into three parts and suppose the standing wave as p'_B and p'_C in the section with liner. Applying the Green's function theory, we can give the standing wave in this part

$$p'_e = p'_B + p'_C = \sum_{m=-\infty}^{\infty}\sum_{n=1}^{N}\left[B_{mn}\psi_m(k_{mn}r)e^{i\gamma^-_{m,n}z} + C_{mn}\psi_m(k_{mn}r)e^{i\gamma^+_{m,n}(z-l)}\right] \tag{18}$$

where B_{mn} and C_{mn} are the amplitudes of the acoustic modes at the interface.

In this work, the effect of uniform liner in circumferential direction on the sound propagation is considered. There is no azimuthal scattering when the sound wave interacts with acoustic treatment. Based on the principle of linear superposition, we can firstly calculate the result of one azimuthal mode interacting with liner. Distinguished from the previous MMA, the expression of standing wave in Eq. (18) includes the eigenvalue and eigenfunction with hard wall instead of impedance wall. In order to acquire the acoustic field in finite domain, it is necessary to build a relationship between scattering sound wave and the standing wave inside the element. Based on the equivalent surface source method, Namba and Fukushige[58] showed that the effect of a liner could be modeled as monopoles with unknown source strength, which naturally avoids the calculation of complex eigenvalues. In fact, the numerical results from this model reveal an excellent agreement with those obtained by using Wiener–Hopf technique. However, due to the complex singularity treatment associated with the observation position close to source point in their model, the equivalent surface source method was not widely applied at that time. In 2007, this method can be developed to calculate the sound propagation with more complex conditions since the singularity can be removed by integral transform method.[59] Therefore, in order to form the solution similar to Eq. (18), the key to the problem is how to solve the integral equation for a finite domain with the same basic assumptions suggested by Namba and Fukushige.[58] For this reason, we are trying to construct the solution by the following steps.

It is mentioned that the vortex wave will propagate through the element without interaction with acoustic treatment, so we do not consider the effect of vortex wave in the liner element. On the other hand, for a monopole source, the generalized Green's function method can be applied to obtaining its solution in the form of

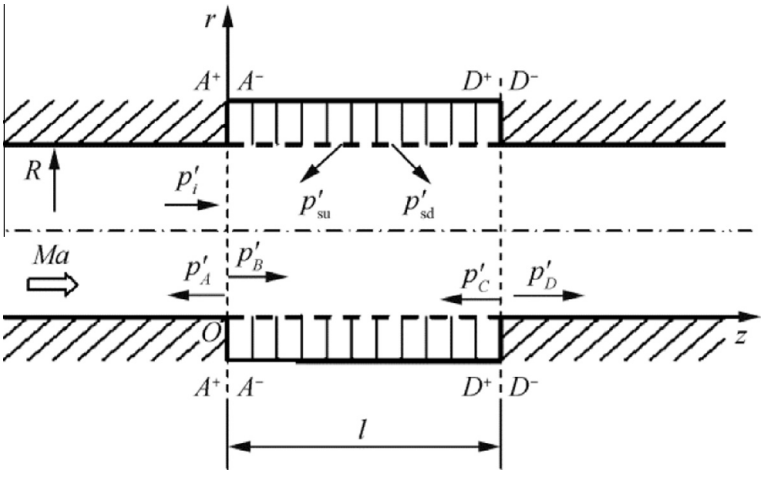

Fig. 8 Geometry of an infinite duct with locally reacting liner.

$$\tilde{p}'_{\mathrm{s}}(\boldsymbol{r},t) = -\int_{-T}^{T}\int_{s(\tau)} \rho_0 \widetilde{V}'_{\mathrm{n}} \frac{\mathrm{D}_0 G}{\mathrm{D}\tau}\mathrm{d}s(\boldsymbol{r}')\mathrm{d}\tau \tag{19}$$

where $\widetilde{V}'_{\mathrm{n}} = V'_{\mathrm{n}} \cdot \mathrm{e}^{\mathrm{i}\omega\tau}$ is the normal velocity at the liner surface $s(\boldsymbol{r})$; G is the Green's function of duct; ρ_0 is the density of flow. On the surface of the liner, standing wave p'_{e}, scattering wave p'_{s} and the impedance Z_{im} must satisfy the boundary condition

$$p'_{\mathrm{s}} + Z_{\mathrm{im}} V_{\mathrm{n}} = -p'_{\mathrm{e}} \tag{20}$$

where V_{n} is acoustic particle velocity. Basing on the displacement continuity condition, V'_{n} can be expressed as

$$V'_{\mathrm{n}} = V_{\mathrm{n}} + \frac{U}{\mathrm{i}\omega}\cdot\frac{\partial V_{\mathrm{n}}}{\partial z'} \tag{21}$$

Combining Eqs. (19)–(21), we can obtain the integral equation of velocity V_{n}. This equation, however, cannot be solved directly because of the unknown coefficient B_{mn} and C_{mn} on the right hand of this integral equation. The disturbance velocity, however, can be rewritten the explicit function of the unknown coefficient. Let

$$V_{\mathrm{n}} = \sum_{k=1}^{\infty} V_k(x',y')\sin\frac{k\pi z'}{l} \tag{22}$$

where l denotes the length of liner.

After handling Eq. (20) by the Fourier sine transform in the region $0 < z < l$, the algebraic equations can be expressed as

$$\sum_{k=1}^{\infty}(z_{jk} + \delta_{jk}Z_{\mathrm{im}})V_k = -I_j, \quad j = 1,2,\ldots \tag{23}$$

where

$$I_j = \sum_{\mu=1}^{N}\psi_m(k_{mn}r)[B_\mu I_j^{B_\mu} + C_\mu I_j^{C_\mu}] \tag{24}$$

The expression of equivalent scattering impedance z_{jk} and Green's function G can be found in Ref. [48]. So the coefficient of V_{n} can be described by

$$V_k = \sum_j \left(z_{jk} + \delta_{jk}Z_{\mathrm{im}}\right)^{-1} I_j = \sum_j \Im_{jk}^{-1} I_j \tag{25}$$

Combine Eqs. (19), (21), (22) and (25), the scattering field can be expressed as

$$\begin{aligned} p'_{\mathrm{s}} &= \sum_{n=1}^{N} p_{dn}\psi_m(k_{mn}r) \\ &= \frac{\rho_0}{2}\sum_{n=1}^{N}\psi_m(k_{mn}r)\mathrm{e}^{\mathrm{i}\gamma^{\pm}_{m,n}z}\left\{\sum_{\mu=1}^{\infty}\left[B_\mu Q_{n\pm}^{B_\mu} + C_\mu Q_{n\pm}^{C_\mu}\right]\right\} \end{aligned} \tag{26}$$

In fact, the solution can be obtained directly when the coefficients of interface wave B_μ and C_μ are known. For Eq. (23), however, the coefficients of acoustic propagation in finite domain are unknown, as shown in Fig. 8. In order to solve the acoustic field in this element, it is necessary to combine the acoustic field inside and outside the element. For that, the matching equations will be built on the interface via continuity of acoustic pressure and acoustic velocity

$$\begin{cases} p'_i + p'_A = p'_B + p'_C + p'_{\mathrm{us}} \\ v'_i + v'_A = v'_B + v'_C + v'_{\mathrm{us}} \end{cases} \tag{27}$$

$$\begin{cases} p'_B + p'_C + p'_{\mathrm{sd}} = p'_D \\ v'_B + v'_C + v'_{\mathrm{sd}} = v'_D \end{cases} \tag{28}$$

where p'_i is sound source; p'_A and p'_D are the sound wave. Due to keeping the eigenvalue of hard wall condition, we can use the orthogonal property to solve the equations. These equations can be rewritten as matrix form

$$\begin{bmatrix} \mathbf{ss}_E^1 & \mathbf{ss}_B^1 & \mathbf{ss}_C^1 & 0 \\ \mathbf{ss}_E^2 & \mathbf{ss}_B^2 & \mathbf{ss}_C^2 & 0 \\ 0 & \mathbf{ss}_B^3 & \mathbf{ss}_C^3 & \mathbf{ss}_D^3 \\ 0 & \mathbf{ss}_B^4 & \mathbf{ss}_C^4 & \mathbf{ss}_D^4 \end{bmatrix} \begin{bmatrix} [A_{m\mu}] \\ [B_{m\mu}] \\ [C_{m\mu}] \\ [D_{m\mu}] \end{bmatrix} = \begin{bmatrix} \boldsymbol{P}_{\mathrm{n}} \\ \boldsymbol{V}_{\mathrm{n}} \\ 0 \\ 0 \end{bmatrix} \tag{29}$$

where $\boldsymbol{P}_{\mathrm{n}}$ and $\boldsymbol{V}_{\mathrm{n}}$ have been transformed from sound source p'_i and v'_i. Each $\mathbf{ss}$ denotes a coefficient matrix. Therefore, for each transfer element, the corresponding matrix can be described as

$$\begin{bmatrix} \mathbf{ss}_B^1 & \mathbf{ss}_C^1 \\ \mathbf{ss}_B^2 & \mathbf{ss}_C^2 \\ \mathbf{ss}_B^3 & \mathbf{ss}_C^3 \\ \mathbf{ss}_B^4 & \mathbf{ss}_C^4 \end{bmatrix}_{4n\times 2n} \tag{30}$$

Until now, the solution in a finite domain with the unknown variables on the interfaces has been constructed. The corresponding matrix expression defined in Eq. (30) is called a "transfer element". More importantly, we will see that the solution for non-locally reacting liner can also be expressed as a transfer element, which remains as the unknown interface parameters. The geometry of non-locally reacting liner is shown in Fig. 9. This kind of perforated liner has attracted great attention mainly due to its potential for various practical applications. In Fig. 9, p_{s}^- and p_{s}^+ denote disturbance acoustic pressure in duct and disturbance acoustic pressure in cavity, respectively. Based on the Green's function, the acoustic field in cavity has been obtained in the form of

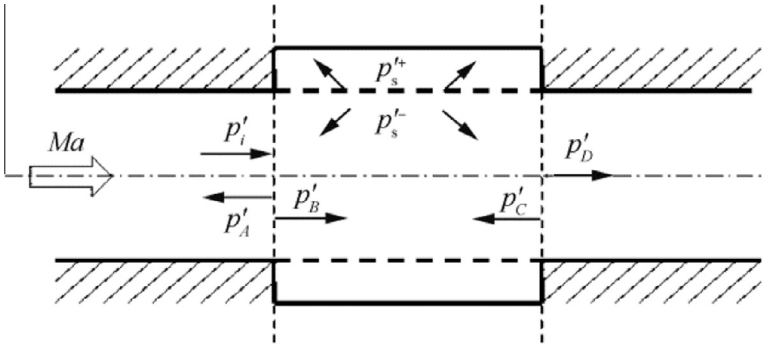

Fig. 9 Geometry of a non-locally reacting liner.

$$p_s^+ = i\rho_0\omega\sum_m\sum_n\sum_q \frac{\psi_m(k_{mn}r)\cos\frac{q\pi z}{l}}{\Gamma_q(k_0^2-k_{m,n,q}^2)}\int_{s(\tau)} V_n\psi_m(k_{mn}r) \times \cos\frac{q\pi z'}{l}dS(\boldsymbol{r}') \tag{31}$$

where $\begin{cases}\Gamma_q = l & q=0\\ \Gamma_q = l/2 & q\neq 0\end{cases}$.

For the scattering wave field in duct p_s^-, it is the same expression as locally reacting liner. As Fig. 9 shows, the acoustic performance of a perforated plate can be depicted as the compliance related to the Rayleigh conductivity c. Hughes and Dowling[60] used Rayleigh conductivity of a single aperture in a plane proposed by Howe[61] to build a smooth compliance for a perforated plate with bias flow. If there is no bias flow, the Rayleigh conductivity can be equivalent to impedance Z_{im} of perforated screen without chamber. Therefore Eq. (20) can be rewritten as

$$p_s'^- - p_s'^+ + Z_{im}V_n = -p_e' \tag{32}$$

For the perforated screen, the same procedure is adopted in this paper. The Rayleigh conductivity equation can be established as

$$p_s'^- - p_s'^+ + \frac{i\omega\rho_0 V_n}{\eta} = -p_e' \tag{33}$$

where η is given by Ref. [48]. In the same way of locally reacting liner, the relevant algebraic equations can be written as

$$\sum_{k=1}^{\infty}\left(z_{jk}^- - z_{jk}^+ + \delta_{jk}\frac{i\omega\rho_0}{\eta}\right)V_k = -I_j,\quad j=1,2,\ldots \tag{34}$$

The expressions of equivalent scattering impedance z_{jk}^+ in the cavity please see Ref. [48]. The same procedure for locally reacting liner as shown in Eq. (23) can be used to solve Eq. (34), i.e., the effect of non-locally reacting liner can also be considered in the present model.

After giving the transfer element for locally and non-locally reacting liner, we can combine these two sections to calculate the sound propagation in Fig. 10.

Based on the transfer element given above, the equations for the combined liner consisting of locally reacting liner and non-locally reacting liner can be written as

$$\begin{bmatrix} \mathbf{ss}_A^{p^+} & \mathbf{ss}_B^{p^-} & \mathbf{ss}_C^{p^-} & & & & \\ \mathbf{ss}_A^{v^+} & \mathbf{ss}_B^{v^-} & \mathbf{ss}_C^{v^-} & & & & \\ & \mathbf{ss}_B^{p^+} & \mathbf{ss}_C^{p^+} & \mathbf{ss}_F^{p^-} & \mathbf{ss}_G^{p^-} & & \\ & \mathbf{ss}_B^{v^+} & \mathbf{ss}_C^{v^+} & \mathbf{ss}_F^{v^-} & \mathbf{ss}_G^{v^-} & & \\ & & & \mathbf{ss}_F^{p^+} & \mathbf{ss}_G^{p^+} & \mathbf{ss}_H^{p} & \\ & & & \mathbf{ss}_F^{v^+} & \mathbf{ss}_G^{v^+} & \mathbf{ss}_H^{v} & \end{bmatrix}\begin{bmatrix}\boldsymbol{A}\\ \boldsymbol{B}\\ \boldsymbol{C}\\ \boldsymbol{F}\\ \boldsymbol{G}\\ \boldsymbol{H}\end{bmatrix} = \begin{bmatrix}\boldsymbol{P}_n\\ \boldsymbol{V}_n\\ 0\\ 0\\ 0\\ 0\end{bmatrix} \tag{35}$$

Solving these equations, we can obtain the acoustic field in both element and entire duct. However, in order to investigate the problem shown as Fig. 7, the acoustic propagation in non-uniform duct has to be considered. According to the result of Alfrdson[62], Gupta et al.[63] and Utsumi[64,65], a slowly varying duct can be approximated by a series of subsections which sides are parallel to the axis of the duct, as shown in Fig. 11(a).

Therefore, for the slowly varying duct, i.e., $\Delta A \ll A$, we can give the matching equations instead of Eq. (27) or Eq. (28) given above, as show in Fig. 11(b),

$$\begin{cases} p_1' + p_1'\frac{U_1^2}{c_1^2} + 2\bar{\rho}_1 U_1 v_1' = p_2' + p_2'\frac{U_2^2}{c_2^2} + 2\bar{\rho}_2 U_2 v_2' \\ \bar{\rho}_1 v_1' + p_1'\frac{U_1}{c_1^2} = \bar{\rho}_2 v_2' + p_2'\frac{U_2}{c_2^2} \\ v_2' = 0 \ \ (\text{for } \Delta A) \end{cases} \tag{36}$$

Before investigating the acoustic problem in Fig. 7, we need to discuss the sound attenuation in lined duct with local reaction liner for validation of the present method. For this purpose, the example given by Rienstra and Eversman[18] has been analyzed and discussed. In this example, "soft-wall" is locally reacting liner with impedance $Z = 2 - i$ on the outer wall within length $0 \leqslant z \leqslant 1.86393$. The specific parameters can be found in Ref. [49]. Besides, the boundary condition suggested previously by Myers[46] and Eversman[66] has been used in the present study. Therefore, considering the variation of mean flow and cross-section of impedance wall, the relationship between the normal velocity V_n' and particle velocity V_n can be rewritten as

$$V_n' = \left[1 + \frac{U_z}{i\omega}\cdot\frac{\partial}{\partial z'} - \left(\sin^2\theta\frac{\partial U_z}{\partial z'} + \sin\theta\cos\theta\frac{\partial U_r}{\partial z'} + \cos^2\theta\frac{\partial U_r}{\partial r}\right)\right]V_n \tag{37}$$

where θ is the axial inclination angle of a non-uniform duct, while velocity U_z and U_r in Eq. (37) include the radial component of the main stream which can be obtained by solving the potential equation. The above equation will reduce to Eq. (21) with uniform flow.

The comparison of acoustic attenuation in various methods has been given in Table 2, in which m is circumferential mode. It is noted that we just use the first order radial mode in hard wall duct as the input sound source in Table 2. The result shows that TEM is an effective method to calculate the sound propagation in non-uniform duct with liner.

In the following text, we will give a more complicated example including the combination of locally reacting and non-locally reacting liners. Especially, with the application

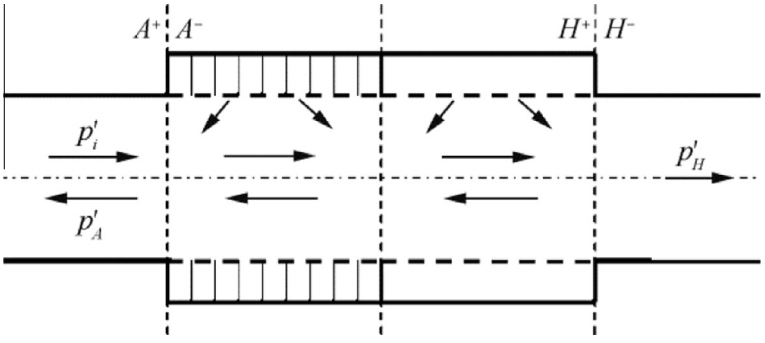

Fig. 10 Illustration of combined liner.

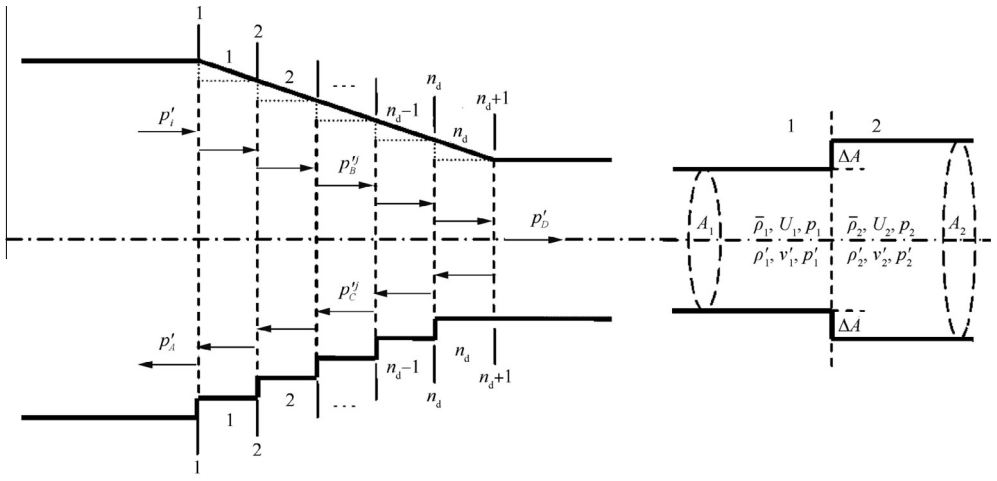

(a) A slowly varying duct (b) Non-uniform cross section

Fig. 11 Configuration for interface matching.

Table 2 Acoustic attenuation comparison of various methods.

Case	m	k_0	Ma	FEM (dB)	MS(dB)	TEM (dB)	Cut-on mode	Cut-off ratio
1a	10	16	0	51.6	51.6	50.4	1	1.36
1b	10	16	−0.5	27.2	27.1	28.1	2	1.25
2a	10	50	0	4.7	3.5	5.9	9	3.38
2b	10	50	−0.5	1.5	0.9	2.7	11	3.97
3a	20	50	0	12.5	12.3	13.3	8	1.91
3b	20	50	−0.5	3.9	3.3	4.7	9	2.26
4a	30	50	0	29.0	28.7	28.4	4	1.34
4b	30	50	−0.5	9.7	8.9	10.7	6	1.59
5a	40	50	0	196	210	182.8	2	1.03
5b	40	50	−0.5	28.4	28.6	29.0	3	1.23

of non-locally reacting liner, the bias flow can be easily induced to go through the plate perforations to realize the adjustment of wall impedance. As we know, the aeroengine works at many different states, such as takeoff, cut back and approach. So, in each case the major noise corresponding to different frequencies and propagating modes needs to be reduced. The locally reacting liner, however, is not suitable to attenuate so many discrete frequency noises simultaneously, as shown in Table 2. It is noted that the sound attenuation is not enough when there are more cut-on modes in the duct, as indicated from the data in the last two columns in Table 2. In fact, a fixed acoustic impedance design is not useful for multi-propagating modes. In these different situations, we can use various combinations of locally and non-locally reacting liners to improve the sound attenuation performance.

As shown in Fig. 7, we use the TEM to calculate the sound propagation in non-uniform duct with local and nonlocal liner. In different situations, the bias flow with Mach number Ma_b is optimized to control the Rayleigh conductivity, as shown in Fig. 12. The geometry parameters and impedance model of local and non-local reaction liners can be found in Ref. [49]. Table 3 gives some numerical results and comparison with a few previous predictions only for the situation with flow.

Even though we only use the short non-local reaction liner instead of the original local reaction liner, the relevant sound

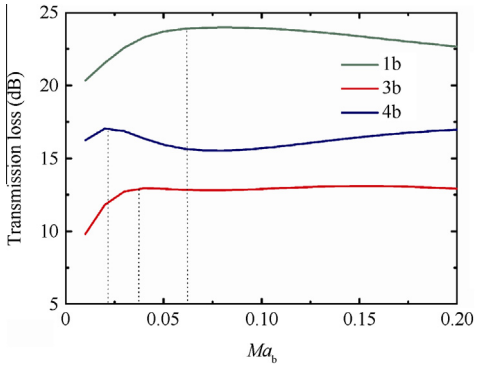

Fig. 12 Effect of bias flow on transmission loss.

Table 3 Comparison of locally reacting liner (TEM) and combined liners.

Case	m	k_0	Ma (z = 0)	Local liner (dB)	Combined liners (dB)
1b	10	16	−0.5	30.0	22.58
2b	10	50	−0.5	2.5	5.29
3b	20	50	−0.5	4.9	12.74
4b	30	50	−0.5	11.2	16.85
5b	40	50	−0.5	31.4	27.35

attenuation could be increased obviously for larger cutoff ratio such as Case 2b, 3b and 4b. The reason is that the bias flow can greatly enhance the resistance and make it optimum in different cases. Of course, there is slightly decrease for smaller cutoff ratio such as Case 1b and 5b, but it is acceptable. Besides, Fig. 12 shows the variation of sound attenuation with the change of bias flow. This means that the frequency range of sound attenuation becomes broader after inducing the bias flow control.

3.2. Interaction between sound source and acoustic liner

As shown in Fig. 1, the acoustic field is very complex in the aeroengine nacelle. Especially, many interactions between various acoustic elements result in the variation of unsteady loading on the blades or vanes, as well as the change of acoustic circumstance that liner is designed for. The current acoustic treatment is designed based on strength-fixed sound source. However, the reaction of the acoustic field in lined duct will inevitably affect the strength of the source, more or less. For the practical problem, the key is how to describe the variation of the unsteady loading on rotor blades and stator vanes with such interactions. In this section we will discuss how to consider the effect of the above factor at the first stage of liner design.

As shown in Fig. 13(a), our purpose is to consider the interaction between sound source and acoustic propagation. In this case it is necessary to set up unified equations including duct liner and rotor/stator vanes. However it is really difficult to solve the sound field generated by unsteady blade loading in a finite domain under the conditions of impedance wall. The main reason is that the Green's function simultaneously including hard wall and soft wall of acoustic propagation cannot be given. Therefore we still need to introduce TEM to solve this problem, as shown in Fig. 13(b). In this method the effects of two different elements on sound generation and propagation will be considered independently. Then the final interaction acoustic field will be solved by establishing matching conditions on the interface. It is different from the previous method[67] because the unified equations will be set up instead of once reflection.

As shown in Fig. 13(b), in order to investigate the interaction between source and liner, it is necessary to establish a sound propagation and generation in a finite domain with blades and liners. In this section we will discuss the TEM for vanes in a finite domain based on the three-dimensional lifting surface theory given by Namba in 1977.[68] The system is three-dimensional with a compressible, inviscid, isentropic and mean flow. The blades have been considered as flat plates of negligible thickness. The mean angle of incidence is zero and the mainstream flow passes through the cascade undeflected.

In order to include the interaction mechanism, we consider two kinds of interaction noise: the first one called the potential interaction caused by pressure waves and cascade, and the second one is generated by the interaction of rotor-wake or vortex waves and the stator vanes. It can be proved that for both wake interaction and potential interaction, the frequency and mode of the scattering field generated by unsteady loading on the vanes will be $f = B\Omega$ and $m = B - qV$, respectively. Where B is the number of circumferential non-uniform of incident source, ω indicates rotating frequency of incident wave, and V expresses the number of vanes. In order to build an independent element which only exchanges information on the interface, we assume that there are several unknown modal pressure waves and modal vortex waves in the section which consists of the interface a–a and d–d and fan stator. As shown in Fig. 14, p'_B, p'_C and w'_B can be expressed as

$$p'_B = \sum_{q=-\infty}^{\infty}\sum_{n=1}^{\infty} B^p_{mn}\cdot\psi_m(k_{mn}r)\cdot e^{i\alpha_1 z} \tag{38}$$

$$p'_C = \sum_{q=-\infty}^{\infty}\sum_{n=1}^{\infty} C^p_{mn}\cdot\psi_m(k_{mn}r)\cdot e^{i\alpha_2(z-l_1)} \tag{39}$$

$$w'_B = \sum_{n=1}^{\infty} B^w_{0n}\cdot\frac{\psi_0(k_{0n}r)}{r}\cdot e^{i\alpha_3 z} \tag{40}$$

where (m, n) represents the circumferential mode and radial mode, respectively. Here $l_1 = l' + b + l''$. The axial wave number α can be expressed as

$$\begin{cases} \alpha_1 = \frac{Ma\cdot k_0 - \sqrt{k_0^2 - \beta^2 k_{mn}^2}}{\beta^2}, & \text{(downstream)} \\ \alpha_2 = \frac{Ma\cdot k_0 + \sqrt{k_0^2 - \beta^2 k_{mn}^2}}{\beta^2}, & \text{(upstream)} \\ \alpha_3 = -\frac{B\Omega}{U}, & \text{(downstream)} \end{cases} \tag{41}$$

The above waves will interact with the fan stator, and consequently the relevant scattering pressure waves p'_s and vortex waves w'_s due to vortex shedding on the trailing edge will be formed. Therefore, we have the following boundary condition on the blade

$$u'_\varphi(r,z) + v'_{B\varphi}(r,z) + v'_{C\varphi}(r,z) + w'_B(r,z) = 0 \tag{42}$$

where $u'_\varphi(r,z)$ represents the normal velocity of scattering field on the blades; $v'_{B\varphi}(r,z)$, $v'_{C\varphi}(r,z)$ and $w'_B(r,z)$ represent the normal velocity of p'_B, p'_C and w'_B on blades, respectively. Therefore, the unsteady loading on the blade is caused by three factors, according to the superposition principle of a linear

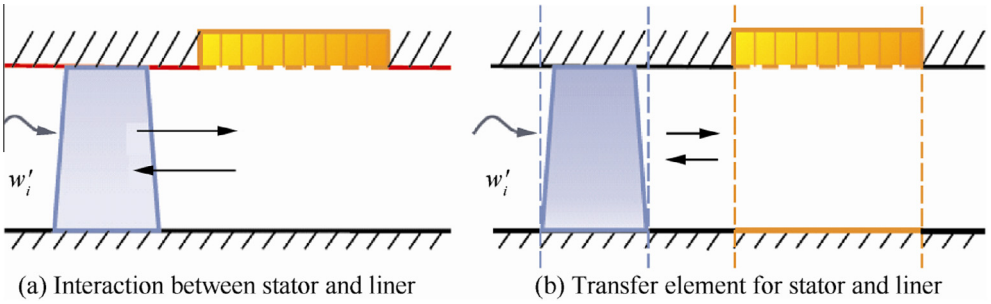

Fig. 13 TEM for investigation between stator and liner.

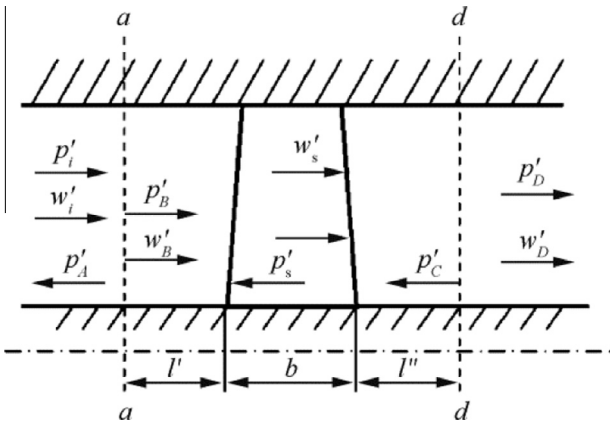

Fig. 14 Transfer element for blades.

system, we can discuss the related unsteady loading caused by these perturbations separately. For example, the unsteady loading $\Delta\bar{p}_1^{\mathrm{w}}$ generated by the interface vortex waves $w'_B(r,z)$ satisfies the boundary condition

$$u'^{\mathrm{w}}_{\varphi}(r,z)+w'_B(r,z)=0 \tag{43}$$

This unsteady loading will result in an acoustic field in transfer element and it can be expressed as

$$p'^{\mathrm{w}}_{\mathrm{s}}(\boldsymbol{x},t)=\int_{-T}^{T}\int_{s(\tau)}\left(\Delta\bar{p}_1^{\mathrm{w}}\right)_i\frac{\partial G}{\partial y_i}\mathrm{d}s(\boldsymbol{y})\mathrm{d}\tau \tag{44}$$

Therefore, in terms of the momentum equation, the normal velocity on the vanes can be acquired by

$$u'^{\mathrm{w}}_{\varphi}(r,z)=\int_0^{\pi}\int_{R_h}^{R_d}\Delta\bar{p}_1^{\mathrm{w}}\cdot\bar{K}_v\mathrm{d}r'\mathrm{d}\theta' \tag{45}$$

The expressions of Green's function G and Kernel function $\bar{K}_v$ can be found in Ref. [50]. Substituting this expression and Eq. (40) into Eq. (43), in the process of solving the integral equation by discretization method, we can obtain the algebraic equations

$$\sum_{i'=1}^{I}\sum_{j'=1}^{J}\Delta\bar{p}^{\mathrm{w}}_{1i'j'}\cdot\bar{K}_{v(ij,i'j')}=-\sum_{n=1}^{N}B^{\mathrm{w}}_{0n}\cdot\frac{\psi_0(k_{0n}r_j)}{r_j}\cdot\mathrm{e}^{\mathrm{i}\alpha_3 z_i} \tag{46}$$

where $\Delta\bar{p}^{\mathrm{w}}_{1i'j'}$ is the vector. There are $I\times J$ orders in the matrix $\bar{K}_{v(ij,i'j')}$. The solution of Eq. (46) is

$$\Delta\bar{p}^{\mathrm{w}}_{1i'j'}=-\sum_{n=1}^{N}B^{\mathrm{w}}_{0n}\sum_{i=1}^{I}\sum_{j=1}^{J}\cdot\left[\bar{K}_{v(ij,i'j')}\right]^{-1}\cdot\frac{\psi_0(k_{0n}r_j)}{r_j}\cdot\mathrm{e}^{\mathrm{i}\alpha_3 z_i} \tag{47}$$

where $[\cdot]^{-1}$ represents the inverse matrix. Let

$$Q^{B^{\mathrm{w}}_n}_{i'j'}=\sum_{i=1}^{I}\sum_{j=1}^{J}\cdot\left[\bar{K}_{v(ij,i'j')}\right]^{-1}\cdot\frac{\psi_0(k_{0n}r_j)}{r_j}\cdot\mathrm{e}^{\mathrm{i}\alpha_3 z_i} \tag{48}$$

and then substitute Eq. (47) into Eq. (44), then $p'^{\mathrm{w}}_{\mathrm{s}}$ can be expressed as

$$p'^{\mathrm{w}}_{\mathrm{s}}(r,z)=\frac{V}{2}\sum_{n'=1}^{N}B^{\mathrm{w}}_{0n'}\sum_{m=-\infty}^{\infty}\sum_{n=1}^{\infty}\frac{m\psi_m(k_{mn}r)}{\kappa_{nm}}$$
$$\int_0^{\pi}\int_{R_h}^{R_d}\frac{Q^{B^{\mathrm{w}}_{n'}}_{i'j'}\psi_m(k_{mn}r')}{r'}\{H(z-z')\mathrm{e}^{\mathrm{i}\alpha_1(z-z')}+H(z'-z)\mathrm{e}^{\mathrm{i}\alpha_2(z-z')}\}\mathrm{d}r'\mathrm{d}\theta' \tag{49}$$

In this expression the scattering wave has been described as explicit function of the incident wave $B^{\mathrm{w}}_{0n'}$ on the interface. In this way we can obtain the sound field generated by interaction between the standing waves or outgoing vortex wave and stator vanes in this element. And then the total acoustic field in this finite domain can be obtained. On the interface plane a–a and d–d, the matching conditions are

$$\begin{cases}p'_i+p'_A=p'_B+p'_C+p'_{\mathrm{s}}\\ v'_i+v'_A=v'_B+v'_C+v'_{\mathrm{s}}\\ w'_i=w'_B\end{cases} \tag{50}$$

$$\begin{cases}p'_B+p'_C+p'_{\mathrm{s}}=p'_D\\ v'_B+v'_C+v'_{\mathrm{s}}=v'_D\\ w'_B+w'_{\mathrm{s}}=w'_D\end{cases} \tag{51}$$

where only p'_i and v'_i are known, while p'_A, p'_D and w'_D can be expanded as

$$p'_A=\sum_{q=-\infty}^{\infty}\sum_{n=1}^{\infty}A^p_{mn}\cdot\psi_m(k_{mn}r)\cdot\mathrm{e}^{\mathrm{i}\alpha_2 z} \tag{52}$$

$$p'_D=\sum_{q=-\infty}^{\infty}\sum_{n=1}^{\infty}D^p_{mn}\cdot\psi_m(k_{mn}r)\cdot\mathrm{e}^{\mathrm{i}\alpha_1(z-l_1)} \tag{53}$$

$$w'_D=\sum_{n=1}^{\infty}D^w_{0n}\cdot\frac{\psi_0(k_{0n}r)}{r}\cdot\mathrm{e}^{\mathrm{i}\alpha_3(z-l_1)} \tag{54}$$

Combining Eqs. (50) and (51), the linear algebraic equations can be solved by the point matching method or the integral transform method. In this paper the alternative transform method based on orthogonal property of eigenfunction in the annular duct with hard wall is chosen by its high accuracy. Therefore we can rewrite the equation as the following matrix forms:

$$\begin{bmatrix}\mathbf{ss}_A^{p_{b-b}} & \mathbf{ss}_B^{p_{b-b}} & \mathbf{ss}_C^{p_{b-b}} & \mathbf{ss}_{w_B}^{p_{b-b}} & \mathbf{0} & \mathbf{0}\\ \mathbf{ss}_A^{v_{b-b}} & \mathbf{ss}_B^{v_{b-b}} & \mathbf{ss}_C^{v_{b-b}} & \mathbf{ss}_{w_B}^{v_{b-b}} & \mathbf{0} & \mathbf{0}\\ \mathbf{0} & \mathbf{0} & \mathbf{0} & \mathbf{ss}_{w_B}^{w_{b-b}} & \mathbf{0} & \mathbf{0}\\ \mathbf{0} & \mathbf{ss}_B^{p_{c-c}} & \mathbf{ss}_C^{p_{c-c}} & \mathbf{ss}_{w_B}^{p_{c-c}} & \mathbf{ss}_D^{p_{c-c}} & \mathbf{0}\\ \mathbf{0} & \mathbf{ss}_B^{v_{c-c}} & \mathbf{ss}_C^{v_{c-c}} & \mathbf{ss}_{w_B}^{v_{c-c}} & \mathbf{ss}_D^{v_{c-c}} & \mathbf{0}\\ \mathbf{0} & \mathbf{ss}_B^{w_{c-c}} & \mathbf{ss}_C^{w_{c-c}} & \mathbf{ss}_{w_B}^{w_{c-c}} & \mathbf{0} & \mathbf{ss}_{w_D}^{w_{c-c}}\end{bmatrix}\begin{bmatrix}\boldsymbol{A}^p_{mn}\\ \boldsymbol{B}^p_{mn}\\ \boldsymbol{C}^p_{mn}\\ \boldsymbol{B}^{\mathrm{w}}_{0n}\\ \boldsymbol{D}^p_{mn}\\ \boldsymbol{D}^{\mathrm{w}}_{0n}\end{bmatrix}=\begin{bmatrix}\boldsymbol{I}^p_{mn}\\ \boldsymbol{I}^v_{mn}\\ \boldsymbol{I}^{\mathrm{w}}_{0n}\\ \mathbf{0}\\ \mathbf{0}\\ \mathbf{0}\end{bmatrix} \tag{55}$$

where $\begin{bmatrix}A^p_{mn} & B^p_{mn} & C^p_{mn} & B^{\mathrm{w}}_{0n} & D^p_{mn} & D^{\mathrm{w}}_{0n}\end{bmatrix}^{\mathrm{T}}$ are unknowns, while $\begin{bmatrix}I^p_{mn} & I^v_{mn} & I^{\mathrm{w}}_{0n} & 0 & 0 & 0\end{bmatrix}^{\mathrm{T}}$ is given by source which can come from anywhere even in the stator element. For the coefficient matrix, superscript p, v and w describe the matching relations of acoustic pressure, acoustic velocity and vortex velocity from the interface plane a–a and d–d, respectively, and the subscripts stand for the number of unknowns on the relevant interface planes. Each **ss** represents a $M\times N$ matrix.

Up to now, a transfer element consisting of Eq. (55) has been constructed. It is easy to see that various element can be combined easily by applying the interface matching conditions. The transfer element matrix for stator vans can be expressed as

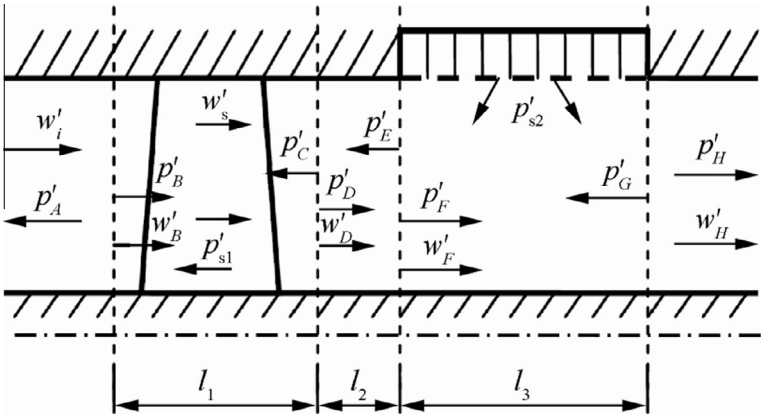

Fig. 15 Illustration of multi-sections.

$$\begin{bmatrix} \mathbf{ss}_B^{p_{b-b}} & \mathbf{ss}_C^{p_{b-b}} & \mathbf{ss}_{w_B}^{p_{b-b}} \\ \mathbf{ss}_B^{v_{b-b}} & \mathbf{ss}_C^{v_{b-b}} & \mathbf{ss}_{w_B}^{v_{b-b}} \\ \mathbf{0} & \mathbf{0} & \mathbf{ss}_{w_B}^{w_{b-b}} \\ \mathbf{ss}_B^{p_{c-c}} & \mathbf{ss}_C^{p_{c-c}} & \mathbf{ss}_{w_B}^{p_{c-c}} \\ \mathbf{ss}_B^{v_{c-c}} & \mathbf{ss}_C^{v_{c-c}} & \mathbf{ss}_{w_B}^{v_{c-c}} \\ \mathbf{ss}_B^{w_{c-c}} & \mathbf{ss}_C^{w_{c-c}} & \mathbf{ss}_{w_B}^{w_{c-c}} \end{bmatrix}. \tag{56}$$

Obviously, this element matrix can also be combined to solve sound propagation in the blade rows. If there are a few different elements which include different effects on the sound propagation, we can set up matrix equations, in which Eq. (56) is element matrix. Combining this element matrix with the transfer element for acoustic treatment as given above, we can obtain the equations to investigate the interactions between these two kinds of acoustic element. It is supposed that there is no interaction between vortex wave and liner. For example, as shown in Fig. 15, the equations are given

It is noted that the existing acoustic design methods for aeroengine nacelle is based on the assumption that the strength of the sound source is fixed without including the interaction between the acoustic treatment and rotor/stator noise source. Furthermore, once the interaction is considered, it is obvious that the strength of the acoustic source will be changed by the presence of the acoustic liner, more or less. Under this circumstance, this means that the noise attenuation not only depends on the acoustic treatment itself but also its interaction with the unsteady loading on the stator vanes or rotor blades. Therefore, a good liner design method needs to include the interaction between sound source and acoustic treatment. However, if we want to consider this coupling, the design of acoustic treatments will face more challenges compared to a strength-fixed sound source. In this paper, the TEM described above has been used to discuss how to obtain more sound attenuation by adjusting the space between fan stator and liner shown in Fig. 15. Some details can be found in Ref. [50]. Fig. 16 shows the variation of SWL with the acoustic resistance for a

$$\begin{pmatrix} \mathbf{ss}_A^{p_{a-a}} & & & & & & & & \\ \mathbf{ss}_A^{v_{a-a}} & & & & & & & & \\ & B & - & C & & & & & \\ & & & & \mathbf{ss}_D^{p_{d-d}} & \mathbf{ss}_E^{p_{d-d}} & \mathbf{0} & & \\ & & & & \mathbf{ss}_D^{v_{d-d}} & \mathbf{ss}_E^{v_{d-d}} & \mathbf{0} & & \\ & & & & \mathbf{0} & \mathbf{0} & \mathbf{ss}_{w_D}^{w_{d-d}} & & \\ & & & & \mathbf{ss}_D^{p_{e-e}} & \mathbf{ss}_E^{p_{e-e}} & \mathbf{0} & & \\ & & & & \mathbf{ss}_D^{v_{e-e}} & \mathbf{ss}_E^{v_{e-e}} & \mathbf{0} & & \\ & & & & \mathbf{0} & \mathbf{0} & \mathbf{ss}_{w_D}^{w_{e-e}} & & \\ & & & & & & & F - G & \mathbf{ss}_H^{p_{h-h}} \\ & & & & & & & & \mathbf{ss}_H^{v_{h-h}} \\ & & & & & & & & \mathbf{ss}_{w_H}^{w_{h-h}} \end{pmatrix} \begin{pmatrix} \boldsymbol{A}_{mn}^p \\ \boldsymbol{B}_{mn}^p \\ \boldsymbol{C}_{mn}^p \\ \boldsymbol{B}_{0n}^w \\ \boldsymbol{D}_{mn}^p \\ \boldsymbol{E}_{mn}^p \\ \boldsymbol{D}_{0n}^w \\ \boldsymbol{F}_{mn}^p \\ \boldsymbol{G}_{mn}^p \\ \boldsymbol{F}_{0n}^w \\ \boldsymbol{H}_{mn}^p \\ \boldsymbol{H}_{0n}^w \end{pmatrix} = \begin{pmatrix} \mathbf{0} \\ \mathbf{0} \\ \vdots \\ \boldsymbol{I}_{mn}^p \\ \boldsymbol{I}_{mn}^v \\ \boldsymbol{I}_{0n}^w \\ \vdots \\ \mathbf{0} \\ \mathbf{0} \\ \mathbf{0} \\ \mathbf{0} \\ \mathbf{0} \end{pmatrix} \tag{57}$$

where $B - C$ represents the transfer element matrix for the stator vanes in an annular duct, while $F - G$ stands for the transfer element matrix for the acoustic treatment. If there are more elements, we can use the same way to set up the final matrix equations by applying interface matching conditions.

few small spaces and also for hard wall case, while the latter one is used to make comparative analysis. It is noticed that there are two propagating modes in this example. As shown in Fig. 16, the optimum sound attenuation comes from the case $l = b$ instead of the case for longer distance $l = 2b$ that

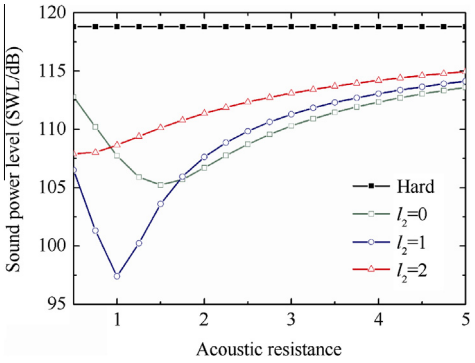

Fig. 16 Effect of fan stator on optimization of acoustic liner.

we usually thought. It is noted that the corresponding noise reduction in the case $l = b$ is nearly two times higher than in the case $l = 2b$. On the other hand, the optimum resistance deeply depends on the space between stator and liner. There is obvious difference for various cases. Therefore, it can be further concluded that the interaction between the fan stator and acoustic treatment is one of major design parameters in sound attenuation.

One of the purposes of the present survey is to reveal the significance of interaction between sound source and acoustic treatment and the advantage of the TEM. Therefore, as shown in Fig. 17, we extend our model to more complex example which includes two acoustic liners installed on the front and aft of the fan stator, respectively. In order to simplify the problem, in this case we suppose that both liners have the same length and resistance. It is also assumed that the space between these two liners and fan stator is fixed, and the other parameters are described in Fig. 15.

Fig. 18 shows the computational result of upstream sound energy with the variation of acoustic resistance for three cases corresponding to Fig. 17. In Fig. 17(b) there is a slight effect on the upstream sound wave, because the coupling is not strong in this situation. However, the comparison between Fig. 17(a) and (c) reveals that the effect of the aft acoustic liner is intensively strong on the upstream sound wave. There are two reasons to explain this phenomenon: the first one is that more downstream sound energy has been reflected to upstream, and in this case the front liner is not good at the reflection field; the second reason is the reflection sound wave strongly influences the unsteady loading, along with more sound energy generation. So, it is not independent for the design of the front and aft acoustic treatments of vane stator and the design of optimal noise reduction should consider the interaction between these elements. Furthermore, an effective design strategy of acoustic liners should include the effect of various interaction mechanisms on the sound generation and propagation in order to optimize the sound attenuation in a wider range of design variables.

3.3. Effect of finite-length duct on liner design

As mentioned above, we want to calculate the noise generation in, sound propagation in and sound radiation from aeroengine duct, as shown in Fig. 1. The interaction between various acoustic elements has been expected to be included in the preliminary liner design. In the previous section, based on the

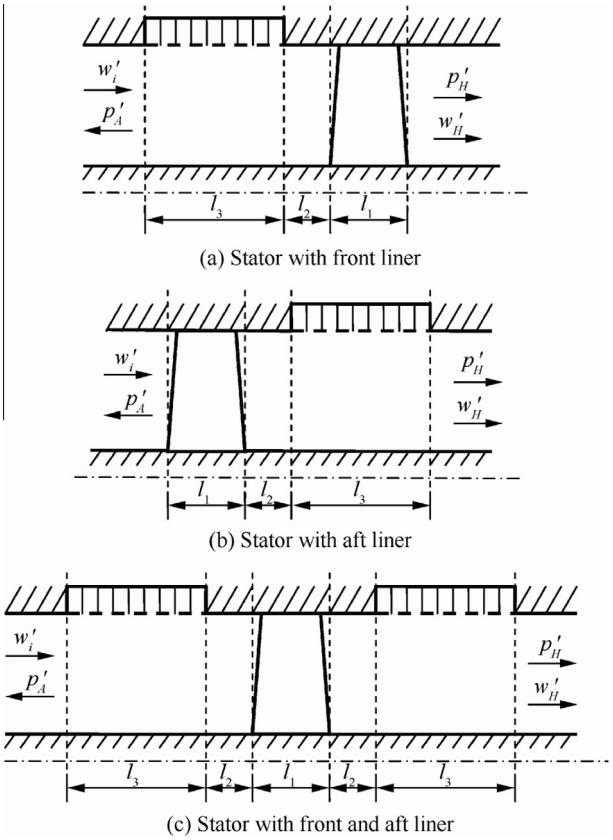

Fig. 17 Schematic of various element combinations.

transfer elements of local and non-local liner and stator vanes, we have discussed the interaction between sound source and various liners. In this section, in order to emphasize the sound radiation from duct, i.e., the effect of the inlet and outlet of an aeroengine nacelle on the liner design, the problem about sound radiation from a duct which is shown in Fig. 19 will be investigated. Regarding the sound source as rotating point source and only considering local reaction liner, the sound radiation model can be established in this section. It is noticed that all the transfer elements that have been given above can be combined with the model in this section to solve the problem about sound radiation as shown in Fig. 1.

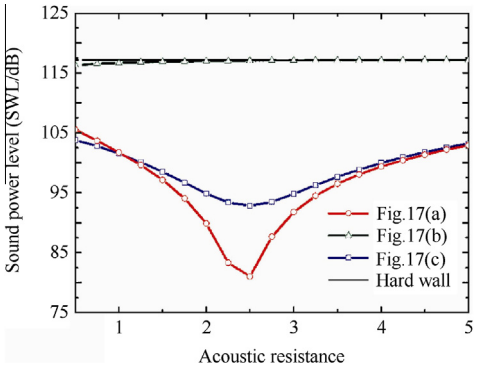

Fig. 18 Comparison of the three cases.

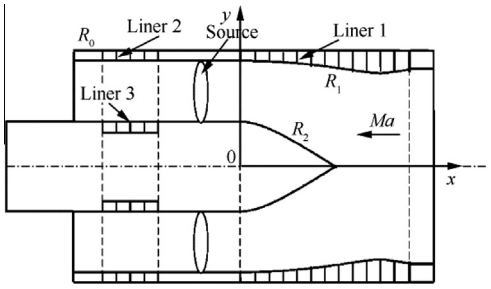

Fig. 19 Schematic of sound radiation of aeroengine.

In this consideration, the BIEM is applied to predicting sound radiation from a finite-length duct, as shown in Fig. 20. Combining the TEM and BIEM, the solving equation including the sound wave inside and outside duct simultaneously has been established, which naturally avoids the requirement for the mode reflection coefficients like MMA. Based on Green's function, the sound radiation from the duct can be obtained in the integral form of

$$C(P)p(P) = \int_S \left[p(Q)\frac{\partial G(P,Q)}{\partial n} - \frac{\partial p(Q)}{\partial n}G(P,Q)\right]\mathrm{d}S(Q) \tag{58}$$

where P, Q are points on the surface S; n is outwards normal direction at a point on the surface, and p is the surface pressure. The function G is the free-space Green's function. We have

$$\begin{cases} C(p) = 0, & \text{for } P \text{ in duct} \\ C(p) = 1, & \text{for } P \text{ out of duct} \\ C(p) = 0.5, & \text{for } P \text{ on a smooth surface of duct} \end{cases} \tag{59}$$

Utilizing the expansion of the boundary conditions and the surface distribution functions in Fourier series with respect to the angle of revolution in the axisymmetric duct, the surface integral of Eq. (58) is reduced to a line integral equation along the duct,[69] as shown in Fig. 20. Discretizing boundary integral Eq. (58), $2M_1 + M_2$ algebraic equations can be obtained

$$\begin{cases} c(P_j)p_{mj} - \sum_{n=1}^{N_e}\sum_{a=1}^{3} p_{mna}A^a_{mnj} + \sum_{n=1}^{N_e}\sum_{a=1}^{3} p^n_{mna}C^a_{mnj} = 0 \\ j = 1, 2, \ldots, 2M_1 + M_2, \quad N_e = 2M_1 + M_2 - 3 \end{cases} \tag{60}$$

The details about discretization approach can be found in Ref. [48]. Here, the method mentioned in Ref. [48] is used to obtain the correlative coefficient matrixes $A^a_{mnj}, C^a_{mnj}\cdot p_{mna}$ and p^n_{mna} are the values of p, $\partial p/\partial n$ at the ath node of nth element for mth circumferential modes. For the situation with mean flow, we can use the transform function $\Psi(x, y, \zeta)$ instead of the previous function $p(x, y, z)$ in Eq. (58). Here, $p(x, y, z) = \Psi(x, y, \zeta)\mathrm{e}^{\mathrm{i}k'_0 Ma\cdot\zeta}, k'_0 = k_0/\beta, z = \beta\zeta$. The new equation can also be solved by Eq. (60) to get the values of $\Psi, \partial\Psi/\partial z$. Obviously, to obtain the values of these unknowns in Eq. (60), $2M_1$ equations have to be constructed to complement the amount of equations in Eq. (60) where only $2M_1 + M_2$ equations are available.

In the model of sound radiation from aeroengine duct, combining the TEM and the BEM, the n_d sections, i.e., $n_\mathrm{d} + 1$ interfaces, have been considered, as shown in Fig. 21. The interior surface of wall in each section can include different boundary conditions, such as rigid wall, local reaction liner and non-local reaction liner. Especially the sound source, such as rotor blade and stator vanes, can also be included in the segment of duct. So based on TEM, the algebraic equations can be obtained

$$\underbrace{\begin{bmatrix} \mathrm{ss}^{2-}_{B_p} & \mathrm{ss}^{2-}_{C_p} & \mathrm{ss}^{2+}_{B_p} & \mathrm{ss}^{2+}_{C_p} & & & & & & \\ \mathrm{ss}^{2-}_{B_v} & \mathrm{ss}^{2-}_{C_v} & \mathrm{ss}^{2+}_{B_v} & \mathrm{ss}^{2+}_{C_v} & & & & & & \\ & & \mathrm{ss}^{3-}_{B_p} & \mathrm{ss}^{3-}_{C_p} & \cdots & & & & & \\ & & \mathrm{ss}^{3-}_{B_v} & \mathrm{ss}^{3-}_{C_v} & \cdots & & & & & \\ & & & & \cdots & \mathrm{ss}^{(n_\mathrm{d}-1)+}_{B_p} & \mathrm{ss}^{(n_\mathrm{d}-1)+}_{C_p} & & & \\ & & & & \cdots & \mathrm{ss}^{(n_\mathrm{d}-1)+}_{B_v} & \mathrm{ss}^{(n_\mathrm{d}-1)+}_{C_v} & & & \\ & & & & & \mathrm{ss}^{n_\mathrm{d}-}_{B_p} & \mathrm{ss}^{n_\mathrm{d}-}_{C_p} & \mathrm{ss}^{n_\mathrm{d}+}_{B_p} & \mathrm{ss}^{n_\mathrm{d}+}_{C_p} \\ & & & & & \mathrm{ss}^{n_\mathrm{d}-}_{B_v} & \mathrm{ss}^{n_\mathrm{d}-}_{C_v} & \mathrm{ss}^{n_\mathrm{d}+}_{B_v} & \mathrm{ss}^{n_\mathrm{d}+}_{C_v} \end{bmatrix}}_{2(n_\mathrm{d}-1)M_1 \times 2n_\mathrm{d}M_1} \begin{bmatrix} B^1 \\ C^1 \\ \vdots \\ B^{n_\mathrm{d}} \\ C^{n_\mathrm{d}} \end{bmatrix} = \underbrace{\begin{bmatrix} 0 \\ \vdots \\ pp_i^{n+} \\ vv_i^{n+} \\ pp_i^{(n+1)-} \\ vv_i^{(n+1)-} \\ \vdots \\ 0 \end{bmatrix}}_{2(n_\mathrm{d}-1)M_1} \tag{61}$$

The vector on the right side is related to the sound source which can come from any section in finite duct. As mentioned above, there are $2M_1 + M_2$ equations in Eq. (60) for exterior sound field of duct and $2(n_\mathrm{d} - 1)M_1$ algebraic equations in Eq. (61) for interior sound field of duct. Based on the p and $\partial p/\partial n$ continuity conditions on the inlet and outlet cross-section, $4M_1$ equations can be constructed.

$$\begin{bmatrix} BB^{1-}_{p} & AA^{1+}_{Bp} & AA^{1+}_{Cp} & & \\ BB^{1-}_{p^n} & AA^{1+}_{Bp^n} & AA^{1+}_{Cp^n} & & \\ & AA^{(n_\mathrm{d}+1)-}_{Bp} & AA^{(n_\mathrm{d}+1)-}_{Cp} & CC^{(n_\mathrm{d}+1)+}_{p} & \\ & AA^{(n_\mathrm{d}+1)-}_{Bp^n} & AA^{(n_\mathrm{d}+1)-}_{Cp^n} & CC^{(n_\mathrm{d}+1)+}_{p^n} & \end{bmatrix}_{4M_1 \times 6M_1} = \begin{bmatrix} pp^{1+}_{ip} \\ pp^{1+}_{ip^n} \\ pp^{(n_\mathrm{d}+1)-}_{ip} \\ pp^{(n_\mathrm{d}+1)-}_{ip^n} \end{bmatrix}_{4M_1 \times 1} \tag{62}$$

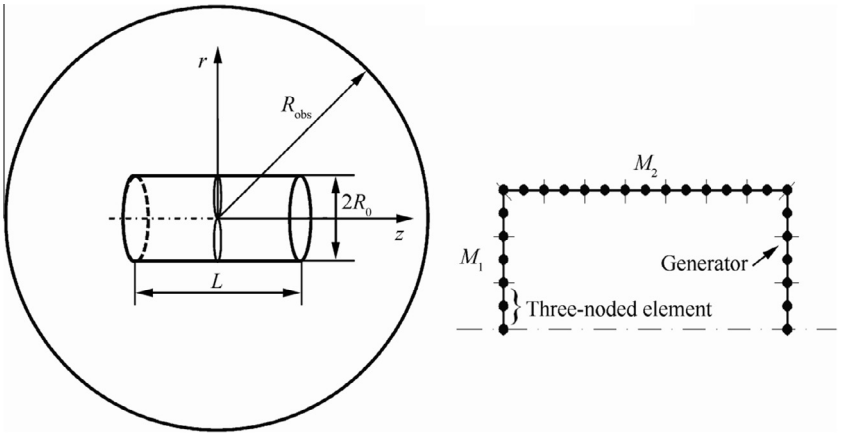

Fig. 20 Geometry of duct and observation point.

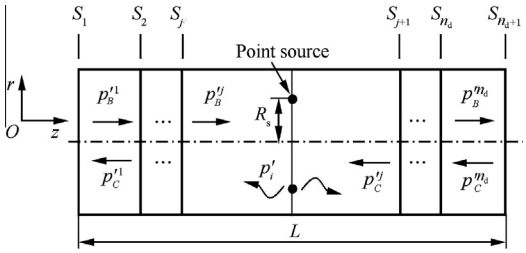

Fig. 21 Geometry of a finite duct with n_d transfer elements.

Solving the linear equations constructed by combining Eqs. (60)–(62), the $(4+2n_d)M_1+M_2$ unknowns will be determined, which means the sound boundary condition of the duct and the acoustic field can be obtained.

It is easy to see that the sound generation in, propagation through and generation from duct can be solved by using TEM and BEM. Here, two examples will be given to investigate the acoustic problem.

As shown in Fig. 22, firstly, the sound radiation from finite duct with local and non-local reaction liners has been investigated via the example given by Dunn et al.[11] which replaces the locally reacting liner with non-locally reacting liner.

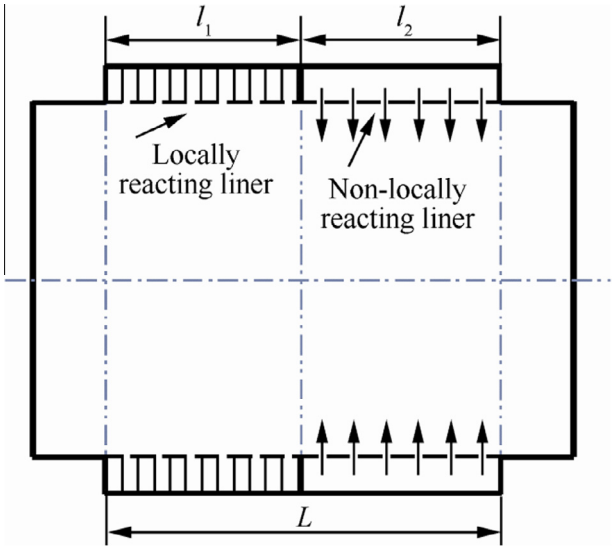

Fig. 22 Sketch of segmented liners.

As shown in Fig. 23 there is an obvious difference when the bias flow exists in the non-locally reacting liner. The present results show that the TEM has obvious advantages over the BIEM and FEM for the far acoustic field when the non-locally reacting liner is used. This kind of liner is particularly efficient for sound attenuation in different states of aeroengine, as mentioned above.

Finally we will give an example about the acoustic radiation from finite duct with acoustic treatment, which is closer to the real situation that aeroengine generates sound radiation than the previous model. As shown in Fig. 19, in this simplified model the sound source is considered as spinning point dipole source. The length of duct with inlet liner 1 $(Z_1=(2,-1), x\in(0,1.86393))$ and exhaust liner 2 and 3 $(Z_2=Z_3=(2,-1), x\in(-1.5,-0.5))$ is 2 m. The

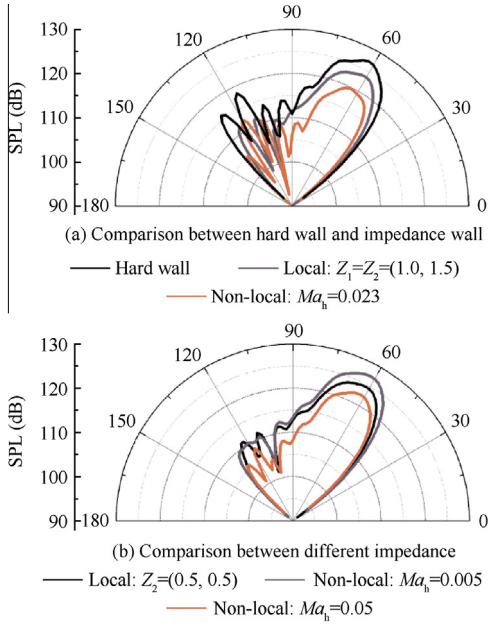

Fig. 23 Sound pressure level on surface of a hemisphere whose radius is equal to 10 m.

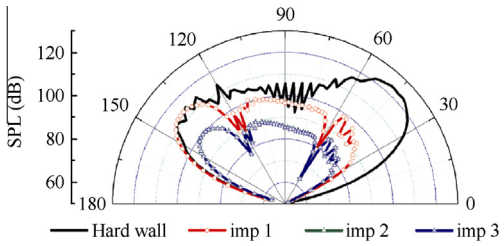

Fig. 24 Effect of liner on sound radiation.

frequency of spinning point dipole source at position $x_i = -0.25$ is 865.8 Hz. The source is described by the following formula:

$$p_i = -\frac{BF_T}{2}\sum_{m=-\infty}^{\infty}\sum_{n=1}^{\infty}\frac{\phi_{mn}(k_{mn}r)\mathrm{e}^{-\mathrm{i}m\varphi}e^{\mathrm{i}\gamma_{mn}^{\pm}z}}{\Gamma_{mn}}\frac{\gamma_{mn}^{\pm}}{\kappa_{mn}}\phi_{mn}(k_{mn}r_1) \qquad (63)$$

where $r_1 = 0.9, F_T = 50$. The outer radius R_1 and inner radius R_2 inside the duct are represented as

$$R_1 = \begin{cases} 1 & x \in (-2,0) \\ 1 - 0.18453x'^2 + 0.10158\frac{\mathrm{e}^{-11(1-x')} - \mathrm{e}^{-11}}{1-\mathrm{e}^{-11}} & x \in (0,1.86393) \\ 1 - 0.18453 - 0.10158\frac{\mathrm{e}^{-11}}{1-\mathrm{e}^{-11}} & x \in (1.86393,2) \end{cases}$$

$$R_2 = \begin{cases} 0.64212 - 0.04777^{1/2} & x \in (-2.6,0) \\ \max[0, 0.64212 - (0.04777 + 0.98234x')^{1/2}] & x \in (0,1.86393) \\ 0 & x \in (1.86393,2) \end{cases}$$

where $x' = x/1.86393$. The outer radius of duct is $R_0 = 1.02$ m and the radiation radius is $r = 10$ m.

In Fig. 24, "Hard wall" expresses hard inlet and hard exhaust; imp1 represents there is only liner 1 in aeroengine duct; "imp2" includes the liner 1 and liner 2; "imp3" denotes that all of the liners exist in Fig. 19. The result plotted in Fig. 24 shows the effect of acoustic treatment on the sound radiation. The inlet noise has been reduced substantially due to the liner 1, but the exhaust noise has been enhanced slightly due to the reflection effect of liner 1 by considering the interaction between the inlet and outlet interfaces. When the exhaust liner exists, the sound radiation is reduced in both inlet and outlet directions.

However, comparing the case "imp2" with the case "imp3", it is found that the difference is very slight due to the absence of liner optimization and spinning flow. On the other hand, the effect of liner 3 on the sound attenuation is small when the hub-tip ratio is less than 0.5, so it is possible that the radiation results of both situations are almost similar.

Once again, the advantage of TEM has been introduced in this paper, but how to realize an optimal acoustic design of aeroengine nacelle still requires considerable work along with the TEM's application.

4. Concluding remarks

In this survey, a kind of new method, TEM, has been introduced with emphasis on its various applications in the sound generation, propagation and radiation in aeroengine. As a new tool for the acoustic design of aeroengine nacelle, it has certain advantages over the existing methods. Especially, the problems associated with the interaction between source and acoustic treatment, the interaction between various liners and the radiation of sound from aeroengine can be analyzed and discussed, and the relevant liner optimization can also be implemented by means of TEM.

Three kinds of example reveal the property and capability of the TEM for evaluating acoustic problems in the aeroengine nacelle. The investigation of a few couplings mechanism shows that the efficiency of acoustic treatment greatly depends on the interaction between incident and ambient sound field. Therefore, the effect of interaction on acoustic liner design has to be considered when the liner exists under a complex acoustic circumstance. Finally, as a fast algorithm, the TEM including more factors of the liner design can be easily applied in practical engineering problem.

Acknowledgements

The authors are grateful to the National Natural Science Foundation of China (No. 51106005), and acknowledge the National Basic Research Program of China (2012CB720201).

References

1. Envia E. Emerging community noise reduction approaches. *Proceedings of 3rd AIAA atmospheric space environments conference*; 2011 Jun 27-30; Honolulu, Hawaii. Reston: AIAA; 2011.
2. Envia E. Fan noise reduction: an overview. *Proceedings of 39th aerospace sciences meeting & exhibit*; Reno, NV. Reston: AIAA; 2001.
3. Huff D. Noise reduction technologies for turbofan engines. *Proceedings of 35th international congress and exposition on noise control engineering*; 2006 Dec 3–6; Honolulu, Hawaii. Washington, D.C.: NASA; 2006.
4. Bielak G, Premo J, Hersh A. Advanced turbofan duct liner concepts. Washington, D.C.: NASA Langley; 1999. Report No.: NASA/CR-1999-209002.
5. Yu J, Kwan H, Chien E, Ruiz M, Nesbitt E, Uellenberg S, et al. Quiet technology demonstrator 2 intake liner design and validation. *Proceedings of 12th AIAA/CEAS aeroacoustics conference*; 2006 May 5–8; Cambridge, Massachusetts. Reston: AIAA; 2006.
6. Mardjono J, Riou G, Boiteux J. EPSL static tests demonstration of liners noise reduction concepts. *Proceedings of 19th AIAA/CEAS aeroacoustics conference*; 2013 May 23-29; Berlin, Germany. Reston: AIAA; 2013.
7. Smith MJT. *Aircraft noise*. New York: Cambridge University Press; 1989.
8. Tyler JM, Sofrin TG. Axial flow compressor noise studies. *Soc Automotive Eng Trans* 1962;**70**:309–32.
9. Myers MK. Boundary integral formulations for ducted fan radiation calculations. *Proceedings of 33rd aerospace sciences meeting and exhibit*; Reno, NV. Reston: AIAA; 1995.
10. Myers MK. Radiation of sound form a point source in a short duct. Proceedings of 2nd computational aeroacoustics (CAA) workshop on benchmark problems; Hampton, VA. Reston: AIAA; 1997.
11. Dunn MH, Tweed J, Farassat F. The application of a boundary integral equation method to the prediction of ducted fan engine noise. *J Sound Vib* 1999;**277**(5):1019–48.
12. Quaranta E, Drikakis D. Noise radiation from a ducted rotor in a swirling-translating flow. *J Fluid Mech* 2009;**641**:463–73.

13. Choi H, Joo LD. Development of the numerical method for calculating sound radiation form a rotating dipole source in an opened thin duct. *J Sound Vib* 2006;**295**(3):739–52.
14. Ozyoruk Y. Numerical prediction of aft radiation of turbofan tones through exhaust jets. *J Sound Vib* 2009;**325**(1):122–44.
15. Iob A, Arina R. Frequency-domain linearized Euler model for turbomachinery noise radiation through engine exhaust. *AIAA J* 2010;**48**(4):848–58.
16. Astley RJ, Eversman W. Finite element formulations for acoustical radiation. *J Sound Vib* 1983;**88**(1):47–64.
17. Danda RI, Eversman W. Improved finite element modeling of the turbofan engine inlet radiation problem. *J Sound Vib* 1995;**117**(1):109–15.
18. Rienstra W, Eversman W. A numerical comparison between the multiple-scales and finite-element solution for sound propagation in lined flow ducts. *J Fluid Mech* 2001;**437**:367–84.
19. Tam CKW. Computational aeroacoustics: issues and methods. *AIAA J* 1995;**33**(10):1788–96.
20. Tam CKW. Computational aeroacoustics: an overview of computational challenges and applications. *Int J Comput Fluid Dyn* 2004;**18**(6):547–67.
21. Ozyoruk Y, Ahujia V, Long N. Time domain simulation of radiation from ducted fans with liners. *Proceedings of 7th AIAA/CEAS aeroacoustics conference*; Maastricht, The Netherlands. Reston: AIAA; 2001.
22. Li X, Scemel C, Michel U. On the azimuthal mode propagation in axisymmetric duct flows. *Proceedings of 8th AIAA/CEAS aeroacoustics conference*; Breckenridge, Colorado. Reston: AIAA; 2002.
23. Bi WP, Pagneux V, Lafarge D, Auregan Y. An improved multimodal method for sound propagation in nonuniform lined ducts. *J Acoust Soc Am* 2007;**122**(1):280–90.
24. Ingard U, Ising H. Acoustic nonlinearity of an orifice. *J Acoust Soc Am* 1976;**42**(1):6–17.
25. Jing XD, Sun XF. Sound-excited flow and acoustic nonlinearity at an orifice. *Phys Fluids* 2002;**14**(1):268–76.
26. Jing XD, Sun XF. Experimental investigations of perforated liners with bias flow. *J Acoust Soc Am* 1999;**106**(5):2436–41.
27. Jing XD, Sun XF. Effect of plate thickness on impedance of perforated plates with bias flow. *AIAA J* 2000;**38**(9):1573–8.
28. Sun XF, Jing XD, Zhang H, Shi Y. Effect of grazing-bias flow interaction on acoustic impedance of perforated plates. *J Sound Vib* 2002;**254**(3):557–73.
29. Ko SH. Sound attenuation in acoustically lined circular ducts in the presence of uniform flow and shear flow. *J Sound Vib* 1971;**22**(2):193–210.
30. Tester BJ. The propagation and attenuation of sound in lined ducts containing uniform or plug flow. *J Sound Vib* 1973;**28**(2):151–203.
31. Noble B. *Method based on the Wiener–Hopf technique for the solution of partial differential equations*. New York: Pergamon Press; 1956.
32. Zorumski WE. Acoustic theory of axisymmetric multi-sectioned ducts. 1974. Report No.: NASA TR R-419.
33. Eversman W. Computation of axial and transverse wave numbers for uniform two-dimensional duct with flow using a numerical integration scheme. *J Sound Vib* 1975;**41**(2):252–5.
34. Eversman W. Initial values for the integration scheme to compute the eigenvalues for propagation in ducts. *J Sound Vib* 1977;**50**(1):159–62.
35. Sun XF, Du L, Yang V. A homotopy method for determining the eigenvalues of locally or non-locally reacting acoustic liners in flow ducts. *J Sound Vib* 2007;**303**(1–2):277–86.
36. Zorumski WE. Generalized radiation impedance and reflection coefficient of circular and annular ducts. *J Acoust Soc Am* 1973;**54**(6):1667–73.
37. Nayfeh AH, Kaiser JE, Telionis DP. Acoustic of aircraft engine-duct systems. *AIAA J* 1975;**13**(2):130–53.
38. Johnston GW, Ogimoto K. Sound radiation from a finite length unflanged circular duct with uniform axial flow. II. Computed radiation characteristics. *J Acoust Soc Am* 1980;**68**(6):1871–83.
39. Johnston GW, Ogimoto K. Sound radiation from a finite length unflanged circular duct with uniform axial flow. I. Theoretical analysis. *J Acoust Soc Am* 1980;**68**(6):1858–70.
40. Dunn MH, Tweed J, Farassat F. The predictin of ducted fan engine noise via a boundary integral equation method. *Proceedings of 2nd AIAA/CEAS aeroacoustics conference*; State College, PA. Reston: AIAA; 1996.
41. Yang B, Wang TQ. An approach to predict ducted fan noise by boundary integral equation method. *Proceedings of 11th AIAA/CEAS aeroacoustics conference*; Monterey, California. Reston: AIAA; 2005.
42. Astley RG, Eversman W. A finite element method for transmission in non-uniform duct without flow: comparison with the method of weighted residuals. *J Sound Vib* 1978;**57**(3):367–88.
43. Eversman W. Turbofan noise propagation and radiation at high frequencies. 2003. Report No.: NASA CR-2003-212323.
44. Richter C, Thiele F, Li XD, Zhuang M. Comparison of time-domain impedance boundary conditions for lined duct flows. *AIAA J* 2007;**45**(6):1333–45.
45. Tam CKW. Recent advances in computational aeroacoustics. *Fluid Dyn Res* 2006;**38**(9):591–615.
46. Myers MK. On the acoustic boundary condition in the presence of flow. *J Sound Vib* 1980;**71**(3):429–34.
47. Eversman W, Parrett AV. Contributions to the finite element solution of the fan noise radiation problem. *J Sound Vib* 1985;**107**(2):216–23.
48. Sun XF, Wang XY, Du L, Jing XD. A new model for the prediction of turbofan noise with the effect of locally and non-locally reacting liners. *J Sound Vib* 2008;**316**(1–5):50–68.
49. Wang XY, Sun XF. A new segmentation approach for sound propagation in non-uniform lined ducts with mean flow. *J Sound Vib* 2011;**330**(10):2369–87.
50. Wang XY, Sun XF. On the interaction of a fan stator and acoustic treatments using the transfer element method. *Fluid Dyn Res* 2010;**42**(1):1–17.
51. Jing XD, Wang XY, Sun XF. Broadband acoustic liner based on the mechanism of multiple cavity resonance. *AIAA J* 2007;**45**(10):2429–37.
52. Li L, Guo ZH, Zhang CY, Sun XF. A passive method to control combustion instabilities with perforated liner. *Chin J Aeronaut* 2010;**23**(6):623–30.
53. Li L, Sun XF. Effect of vorticity waves on azimuthal instabilities in annular chambers. *Combust Flame* 2014;**162**(3):628–41.
54. Li L, Yang LJ, Sun XF. Effect of distributed heat source on low frequency thermoacoustic instabilities. *J Sound Vib* 2013;**332**(12):3098–111.
55. Sun XF, Sun DK, Liu XH, Yu WW, Wang XY. Theory of compressor stability enhancement using novel casing treatment, Part 1: Methodology. *J Propul Power* 2014;**30**(5):1224–35.
56. Sun XF, Sun DK, Yu WW. A model to predict stall inception of transonic axial flow fan/compressors. *Chin J Aeronaut* 2011;**24**(6):687–700.
57. Liu XH, Sun DK, Sun XF, Wang XY. Flow stability model for fan/compressors with annular duct and novel casing treatment. *Chin J Aeronaut* 2012;**25**(2):143–54.
58. Namba M, Fukushige K. Application of the equivalent surface source method to the acoustics of duct systems with non-uniform wall impedance. *J Sound Vib* 1980;**73**(1):125–46.
59. Wang XY, Sun XF. Evolution of the equivalent source surface. *J Eng Thermophys* 2006;**27**(s1):109–12 Chinese.
60. Hughes IJ, Dowling AP. The absorption of sound by perforated linings. *J Fluid Mech* 1990;**218**:299–335.

61. Howe MS. On the theory of unsteady high Reynolds number flow through a circular aperture. *Proc R Soc Lond A Math Phys Sci* 1979;**366**(1725):205–23.
62. Alfredson RJ. The propagation of sound in a circular duct of continuously varying cross-sectional area. *J Sound Vib* 1972;**23**(4):433–42.
63. Gupta VH, Easwaran V, Munjal ML. A modified segmentation approach for analyzing plane wave propagation in non-uniform ducts with mean flow. *J Sound Vib* 1995;**182**(5):697–707.
64. Utsumi M. An efficient method for sound transmission in non-uniform circular ducts. *J Sound Vib* 1999;**277**(4):735–48.
65. Utsumi M. Sound transmission in circular ducts of continuously varying cross-section area. *J Sound Vib* 2001;**242**(2):369–76.
66. Eversman W. The boundary condition at an impedance wall in a non-uniform duct with potential mean flow. *J Sound Vib* 2001;**246**(1):63–9.
67. Ovenden NC, Rienstra SW. *In-duct matching strategies dissertation*. Eindhoven: Eindhoven University of Technology; 2002.
68. Namba M. Three-dimensional analysis of blade force and sound generation for an annular cascade in distorted flow. *J Sound Vib* 1977;**50**(4):479–508.
69. Wang W, Ataun N, Nicolas J. A boundary integral approach for acoustic radiation of axisymmetric bodies with arbitrary boundary conditions valid for all wave numbers. *J Acoust Soc Am* 1997;**101**(3):1468–78.

Wang Xiaoyu is an assistant at School of Energy and Power Engineering, Beihang University, China. She received the Ph.D. degree from Beihang University in 2010, and then became a lecturer there. Her main research interest is aeroacoustics.

Sun Xiaofeng is a professor at School of Energy and Power Engineering, Beihang University, China. His current research interests are aeroacoustics, combustion instabilities and compressor flow instabilities.